Article

Plasma MTBR-tau243 biomarker identifies tau tangle pathology in Alzheimer's disease

Check for updates

Kanta Horie [1,2,3,13] ✉, Gemma Salvadó [4,13], Rama K. Koppisetti[1,5],
Shorena Janelidze [4], Nicolas R. Barthélemy[1,2], Yingxin He [1,2],
Chihiro Sato [1,2], Brian A. Gordon [6,7], Hong Jiang[2],
Tammie L. S. Benzinger [6,7,8], Erik Stomrud[4,9], David M. Holtzman [2,7,8],
Niklas Mattsson-Carlgren[4,9,10], John C. Morris[2,7], Sebastian Palmqvist [4,9],
Rik Ossenkoppele[4,11,12], Suzanne E. Schindler [2,7], Oskar Hansson [4,13,14] ✉ &
Randall J. Bateman [1,2,7,8,13,14] ✉

Insoluble tau aggregates within neurofibrillary tangles are a defining neuropathological feature of Alzheimer's disease (AD) and closely correlate with clinical symptoms. Although tau pathology can be assessed using tau positron emission tomography, a more accessible biomarker is needed for diagnosis, prognosis and tracking treatment effects. Here we present a new plasma tau species, the endogenously cleaved, microtubule-binding region containing residue 243 (eMTBR-tau243), which specifically reflects tau tangle pathology. Across the AD spectrum in three different cohorts ($n = 108$, 55 and 739), plasma eMTBR-tau243 levels were significantly elevated at the mild cognitive impairment stage and increased further in dementia. Plasma eMTBR-tau243 showed strong associations with tau positron emission tomography binding ($\beta = 0.72$, $R^2 = 0.56$) and cognitive performance ($\beta = 0.60$, $R^2 = 0.40$), outperforming other plasma tau (%p-tau217 and %p-tau205) biomarkers. These results suggest that plasma eMTBR-tau243 may be useful for estimating the tauopathy load in AD, thereby improving the diagnostic evaluation of AD in clinical practice and monitoring the efficacy of tau-targeted therapies in clinical trials.

Amyloid β (Aβ)-targeted immunotherapies can slow cognitive and functional decline by 25–40% in symptomatic individuals with Alzheimer's disease (AD)[1,2]. However, accumulating evidence indicates that such therapies are more effective in symptomatic individuals with lower levels of aggregated tau in the brain[2]. Also, as ~25% of older people have amyloid plaques without symptoms[3], diagnostic tests that measure amyloid plaques do not necessarily indicate that a patient's cognitive impairment is caused by AD. Therefore, biomarkers that quantify the amount of aggregated tau can facilitate identification of patients who have cognitive symptoms caused by AD and indicate the magnitude and likelihood of benefit from anti-Aβ therapies. Furthermore, there is a growing interest in tau-targeted treatments, because tau pathology correlates more strongly with clinical disease progression than amyloid[4,5].

Anti-tau therapies might have additive or synergistic effects when combined with current anti-Aβ therapies and they could potentially benefit many patients with AD who have already passed the therapeutic window for anti-Aβ therapy. However, to be able to effectively develop anti-tau treatments, we need reliable, specific and accessible biomarkers that reflect tau-related pathological changes in AD.

Positron emission tomography (PET) imaging with radioligand binding to the aggregated filament form of tau provides insights into the brain's accumulation of insoluble tau aggregates specific to AD, such as neurofibrillary tangles and neuropil threads[6–8]. Tau-PET imaging studies have revealed a strong correlation between insoluble tau aggregates and cognitive decline, even in the early stages of AD dementia, establishing tau-PET as the most precise prognostic indicator for

Table 1 | Characteristics of participants from the validation cohort

	Overall (n=739)	CU⁻ (n=110)	CU⁺ (n=198)	MCI⁺ (n=169)	AD⁺ (n=134)	Other (n=128)
Age, years	72.4 (9.32)	63.8 (11.5)	74.4 (8.41)	73.8 (7.56)	75.3 (7.41)	72.1 (8.14)
Women, n (%)	371 (50.2)	61 (55.5)	104 (52.5)	79 (46.7)	87 (64.9)	40 (31.3)
Education, years	12.8 (3.75) (n=720)	13.4 (3.41) (n=109)	13.0 (3.65) (n=197)	12.7 (4.11) (n=164)	12.2 (3.63) (n=126)	12.9 (3.78) (n=124)
APOE-ε4, n (%)	388 (52.5) (n=664)	43 (39.1) (n=101)	93 (47.0) (n=139)	122 (72.2) (n=168)	95 (70.9) (n=132)	35 (27.3) (n=124)
Aβ-PET, centiloids	41.5 (48.3) (n=483)	−7.26 (5.98) (n=83)	48.6 (38.3) (n=131)	81.4 (38.9)	97.9 (36.7) (n=19)	−1.69 (19.0) (n=80)
Aβ positivity, n (%)	516 (69.8) (n=732)	0 (0)	198 (100)	169 (100)	130 (97.0) (n=130)	19 (14.8) (n=125)
Tau-PET, Braak I–VI (SUVR)	1.23 (0.321) (n=649)	1.08 (0.0757) (n=104)	1.13 (0.154) (n=175)	1.28 (0.300) (n=144)	1.65 (0.471) (n=105)	1.09 (0.0826) (n=121)
Tau-PET positivity, n (%)	172 (23.3) (n=649)	1 (0.9) (n=104)	22 (11.1) (n=175)	57 (33.7) (n=144)	83 (61.9) (n=105)	9 (7.0) (n=121)
Plasma eMTBR-tau243 (fmol l⁻¹)	2.18 (4.64)	0.0845 (0.0973)	0.520 (1.06)	2.32 (3.17)	8.01 (7.69)	0.244 (0.587)
Plasma %p-tau217 (%)	1.52 (1.24)	0.460 (0.112)	1.24 (0.662)	1.95 (1.06)	3.07 (1.37)	0.640 (0.349)
Plasma %p-tau205 (%)	0.517 (0.273)	0.287 (0.133)	0.437 (0.163)	0.628 (0.231)	0.813 (0.293)	0.383 (0.180)
MMSE	26.1 (4.60) (n=720)	29.0 (1.37) (n=108)	28.8 (1.29) (n=194)	26.2 (2.88) (n=162)	19.5 (5.43) (n=129)	26.1 (3.55) (n=127)

Mean (s.d.) is shown unless otherwise specified. In the cases where some were missing, the final sample size is shown in parentheses. Aβ positivity was assessed using CSF Aβ42/40 or Aβ-PET using previously validated thresholds. Tau-PET positivity was assessed in the global region (Braak I–VI) using a previously validated cutoff (SUVR >1.22). Participants classified as 'other' include: 18 PD or DLB, 6 PSP or CBS, 4 VaD, 2 FTD, 86 MCI⁻ and 12 had another neurodegenerative dementia. SUVR, standardized uptake value ratio.

AD-related symptoms currently available[5,9]. However, the high cost and extensive infrastructure required for PET imaging limit its availability to specialized facilities. In contrast, fluid biomarkers offer greater clinical accessibility and affordability because of their much lower infrastructure requirements, affordability and potential for testing independent of location. The most widely used fluid biomarkers to identify AD pathology are Aβ peptides 40 and 42 (Aβ42/Aβ40 ratio) and tau phosphorylated at residues 181 and 217 (p-tau181, p-tau217 and their ratios to nonphosphorylated tau (%p-tau181 and %p-tau217)) measured in cerebrospinal fluid (CSF) or plasma[10–13]. However, these biomarkers are more associated with amyloid plaques than insoluble tau aggregates[14–16]. For example, levels of CSF and plasma p-tau species are elevated in preclinical AD, many years before extensive insoluble tau aggregates are detectable in the cortex by tau-PET[17,18]. Furthermore, recent clinical trials have shown significant reductions of CSF and plasma p-tau181 and p-tau217 in response to anti-Aβ immunotherapies, which reduced levels of amyloid plaques but had less or no effect on tau aggregates[1,2]. These observations collectively indicate that p-tau181 and p-tau217 species in CSF and plasma do not directly measure insoluble tau aggregates, but instead reflect changes in soluble tau phosphorylation in response to Aβ plaques. Therefore, we recently developed mass spectrometry (MS)-based assays that quantify the levels of p-tau205 and the tau microtubule-binding region containing residue 243 (MTBR-tau243) in CSF[19,20]. We found that CSF MTBR-tau243 is selectively and highly correlated with insoluble tau aggregate pathology, as measured by tau-PET, and less strongly associated with amyloid pathology than other tau species[19]. However, although CSF is more widely available than PET, lumbar puncture requires highly trained personnel and is perceived by some patients as risky or invasive. A blood-based test for aggregated tau would be more acceptable, accessible and scalable, facilitating clinical diagnosis, potentially providing prognostic information on the likelihood of benefit for anti-Aβ therapies and enhancing the efficiency of clinical trials.

In the present study, we developed a new plasma-based assay of endogenously cleaved MTBR-tau243 (eMTBR-tau243). This assay was first tested in two pilot cohorts (n = 108 and n = 55) and subsequently evaluated in a larger clinical cohort, the Swedish BioFINDER-2 study (n = 739), which includes individuals across the entire AD continuum, with Aβ-PET, tau-PET, magnetic resonance imaging (MRI) and cognitive data available. We compared plasma eMTBR-tau243 with plasma %p-tau217 and %p-tau205, which are associated with both Aβ and tau pathologies in AD[12,19,20]. To determine whether plasma eMTBR-tau243 is more specific to AD tau tangle pathology, we examined the plasma biomarkers across various diagnostic groups. Finally, we assessed the associations between the plasma biomarkers and downstream effects of AD pathologies, including brain atrophy and cognitive impairment.

Results

Development of plasma eMTBR-tau243 assay

First, we applied the CSF MTBR-tau243 method previously reported[19] to measure MTBR-tau243 in three matched plasma and CSF samples from individuals with different levels of tau-PET pathological loads (low, medium and high). Tau species were immunoprecipitated and digested with trypsin followed by MS analysis for the tryptic peptide (residues 243–254). We found that the tryptic MTBR-tau243 peptide level was correlated with tau-PET signal for CSF but not for plasma samples (Supplementary Fig. 1). Next, we discovered an eMTBR-tau243 species with carboxy-terminal endogenous cleavage at residue 256 (valine) and deamidation at residue 255 (asparagine), which was proportional to tau-PET in both the plasma and the CSF samples (Supplementary Fig. 2).

Using the newly developed assay, we investigated whether plasma eMTBR-tau243 increases with cognitive symptoms in two pilot cohorts: the Swedish BioFINDER-2 cohort (n = 108) and the Charles F. and Joanne Knight Alzheimer Disease Research Center (Knight ADRC) cohort (n = 55). The pilot BioFINDER-2 cohort included 57 cognitively unimpaired Aβ-negative participants (CU⁻), 4 cognitively unimpaired Aβ-positive participants (CU⁺), 10 mild cognitive impairment (MCI) Aβ-positive participants (MCI⁺) and 37 AD dementia Aβ-positive participants (AD⁺) (Supplementary Table 1). The mean (s.d.) age was 76.1 ± 7.0 years, 53 (49%) were women and 56 (52%) were APOE-ε4 carriers. The pilot Knight ADRC cohort included 15 CU⁻, 14 CU⁺, 18 very mild AD⁺ (Clinical Dementia Rating (CDR) = 0.5), and 8 AD⁺ (CDR = 1+). The mean (s.d.) age was 73.2 ± 6.1 years, 24 (44%) were women and 28 (51%) were APOE-ε4 carriers (Supplementary Table 2).

We compared eMTBR-tau243 levels in plasma between different diagnostic groups. In both pilot BioFINDER-2 and the Knight ADRC cohorts, plasma eMTBR-tau243 levels were significantly increased in AD⁺ compared with MCI⁺ (or very mild AD⁺; P = 0.015 and 0.005, respectively). However, plasma eMTBR-tau243 levels were no different in CU⁺ compared with CU⁻ (P = 0.632 and 0.791, respectively)

(Extended Data Fig. 1a.c), indicating that the measure is not increased by the presence of just amyloid plaques. We also investigated the correlations between plasma eMTBR-tau243 and CSF MTBR-tau243 levels in the pilot BioFINDER-2 and the Knight ADRC cohorts. Plasma eMTBR-tau243 levels were strongly correlated with CSF MTBR-tau243 levels in BioFINDER-2 (Spearman's $\rho = 0.92$ (95% confidence interval (CI) = 0.89–0.94), $P < 0.001$) and the Knight ADRC (0.79 (95% CI = 0.66–0.88), $P < 0.001$; Extended Data Fig. 1b,d).

Differences by diagnosis in the validation cohort

We next measured plasma eMTBR-tau243 levels in the larger BioFINDER-2 validation cohort, which included 739 individuals, completely independent of the pilot cohort. Of these, 110 were CU^-, 198 were CU^+, 86 had MCI without Aβ pathology (MCI^-), 169 had MCI^+, 134 had AD^+, 18 had Parkinson's disease (PD) or Lewy body dementia (DLB), 6 had progressive supranuclear palsy (PSP) or corticobasal syndrome (CBS), 4 were classified as vascular dementia (VaD), 2 had frontotemporal dementia (FTD), 2 were Arg406Trp (R406W) MAPT mutation carriers (one tau-PET positive and the other tau-PET negative) and 12 had other neurodegenerative dementias (Table 1). The mean (s.d.) age was 72.4 (9.3) years, 50.2% were women and 52.5% were APOE-ε4 carriers. Correlations between plasma eMTBR-tau243 and other plasma biomarkers, including %p-tau217 and %p-tau205, are detailed in Extended Data Fig. 2.

We compared plasma biomarker levels across diagnostic groups in the validation cohort. Similar to the pilot cohorts, plasma eMTBR-tau243 levels were significantly higher in patients who were MCI^+ and AD^+ than CU^- ($P < 0.001$ for both) or CU^+ ($P < 0.001$ for both; Fig. 1a and Supplementary Table 3). No significant differences were observed between CU^- and CU^+ ($P = 0.235$), indicating the lack of amyloid pathology-driven, plasma eMTBR-tau243 elevation during presymptomatic stages. However, significant differences were detected between participants who were MCI^+ and MCI^- participants ($P < 0.001$). Notably, plasma eMTBR-tau243 levels were not elevated in non-AD tauopathies and the levels were similar to those in controls in PSP or CBS (primary 4R tauopathies) and in FTD (where some have primary 3R tau pathology). However, one of two MAPT R406W mutation carriers (with mixed 3R/4R tau pathology similar to AD), who was Aβ negative but tau-PET positive with symptoms of FTD, exhibited an elevated plasma eMTBR-tau243 level.

As expected, plasma %p-tau217 levels also increased across the AD continuum (Fig. 1b). However, unlike eMTBR-tau243, %p-tau217 levels were significantly higher in CU^+ than CU^- ($P < 0.001$). Plasma %p-tau205 levels demonstrated a similar trend to %p-tau217, albeit with greater variability across disease stages (Fig. 1c).

Associations with tau-PET in the validation cohort

We evaluated the relationship between plasma biomarkers and tau-PET using linear regression analyses adjusted for age and sex. First, we examined tau-PET-positive individuals, because plasma eMTBR-tau243 levels were expected to increase significantly during the later stages of the disease. Plasma eMTBR-tau243 demonstrated a robust positive correlation with tau pathology as measured by tau-PET in a global cortical region of interest (ROI; Braak I–VI regions) ($\beta = 0.68$ (95% CI = 0.57–0.80), $P < 0.001$, $R^2 = 0.45$; Fig. 2a and Supplementary Table 4). Plasma %p-tau217 and %p-tau205 also exhibited positive associations with tau

pathology (%p-tau217: $\beta = 0.57$ (95% CI = 0.44–0.70), $P < 0.001$, $R^2 = 0.32$ and %p-tau205: $\beta = 0.50$ (95% CI = 0.36–0.64), $P < 0.001$, $R^2 = 0.22$), but their associations were significantly lower than that of plasma eMTBR-tau243 ($P_{diff} \leq 0.002$ in all cases).

Similar findings were observed among Aβ-positive individuals (Fig. 2b and Supplementary Table 4). The strongest association was observed between tau pathology and plasma eMTBR-tau243 ($\beta = 0.74$ (95% CI = 0.68–0.81), $P < 0.001$, $R^2 = 0.54$), which was significantly stronger than the associations with %p-tau217 ($\beta = 0.68$ (95% CI = 0.61–0.75), $P < 0.001$, $P_{diff} < 0.001$, $R^2 = 0.45$) and %p-tau205 ($\beta = 0.60$ (95% CI = 0.52–0.68), $P < 0.001$, $P_{diff} < 0.001$, $R^2 = 0.34$). Results were similar when analyzing all participants, irrespective of Aβ status, as shown in Fig. 2c.

Furthermore, the relationships between plasma %p-tau217 and %p-tau205 with tau-PET differed markedly from that of plasma eMTBR-tau243. Specifically, eMTBR-tau243 showed a more linear correlation with tau-PET, particularly in tau-PET-positive individuals, whereas the relationships for %p-tau217 and %p-tau205 plateaued. Plasma %p-tau217 levels increased with Aβ positivity before tau pathology became detectable on PET. This distinction was also evident in the distribution of data separated into quadrants based on biomarker thresholds (Extended Data Fig. 3). For eMTBR-tau243 in Aβ-positive participants, most individuals were negative on both tau-PET and eMTBR-tau243 (59.2%), followed by those positive for both (29.8%), with minimal discordance (tau-PET-positive/eMTBR-tau243-negative: 4.1%; tau-PET-negative/eMTBR-tau243-positive: 6.9%; Extended Data Fig. 3a). In contrast, plasma %p-tau217 showed a higher proportion of individuals who were plasma positive but tau-PET negative (40.6%). These findings suggest that, although eMTBR-tau243 levels become abnormal around the same time as tau-PET, %p-tau217 becomes abnormal earlier. Plasma %p-tau205 patterns in the distribution of data separated into quadrants were similar to those of eMTBR-tau243.

We further analyzed associations with tau-PET in Aβ-positive individuals using specific ROIs reflecting early (Braak I–II), intermediate (Braak III–IV) and late (Braak V–VI) tau-accumulating regions. For early accumulating regions, the associations of eMTBR-tau243 and %p-tau217 with tau-PET were not significantly different (eMTBR-tau243: $\beta = 0.72$ (95% CI = 0.66–0.79) versus %p-tau217: $\beta = 0.69$ (95% CI = 0.63–0.76), $P_{diff} = 0.147$). However, eMTBR-tau243 showed significantly stronger and more linear correlations with tau-PET in intermediate and late accumulating regions (intermediate region: eMTBR-tau243: $\beta = 0.75$ (95% CI = 0.68–0.81) versus %p-tau217: $\beta = 0.69$ (95% CI = 0.62–0.76), $P_{diff} < 0.001$; and late region: eMTBR-tau243: $\beta = 0.70$ (95% CI = 0.63–0.77) versus %p-tau217: $\beta = 0.64$ (95% CI = 0.56–0.71), $P_{diff} < 0.001$; Extended Data Fig. 4 and Supplementary Table 4). Similar results were observed in tau-PET-positive individuals (Extended Data Fig. 5 and Supplementary Table 4).

To assess the independent contribution of plasma biomarkers, we included all three markers as predictors in a multivariate model, with continuous tau pathology measures as the outcome. Among Aβ-positive participants, plasma eMTBR-tau243 demonstrated the largest effect across all tau-PET regions (global region: eMTBR-tau243: $\beta = 0.50$ (95% CI = 0.39–0.60), $P < 0.001$; %p-tau217: $\beta = 0.18$ (95% CI = 0.07–0.29), $P = 0.002$; %p-tau205: $\beta = 0.12$ (95% CI = 0.03–0.21), $P = 0.008$), which was most pronounced for the intermediate and late cortical regions (Fig. 3 and Supplementary Table 5). These findings suggest that plasma

---

Fig. 1 | Plasma biomarker levels by diagnostic group in the validation cohort demonstrate that plasma eMTBR-tau243 is highly specific for AD compared with other neurodegenerative diseases. a–c, Plasma levels of eMTBR-tau243 (**a**), %p-tau217 (**b**) and %p-tau205 (**c**) by clinical diagnosis and Aβ status in the main BioFINDER-2 cohort ($n = 739$). Statistical differences were assessed using ANCOVA adjusted for age and sex followed by Tukey's corrected, post hoc pairwise comparisons (two-sided analysis). Dots are gray color coded to indicate tau-PET negativity in the global (Braak I–VI) ROIs whereas white color-coded dots indicate tau-PET data that are not available and other color-coded dots indicate tau-PET positivity. MAPT R406W mutation carriers are shown in pink (one FTD who is tau-PET positive and one MCI^- who is tau-PET negative). Plasma thresholds were derived using Gaussian mixture modeling. Percentage of Aβ- and tau-positive individuals are included in each group. Aβ status was assessed using CSF Aβ42/40 or Aβ-PET and tau status with a global tau-PET (SUVR > 1.22). Boxplots summarize data distribution, showing the median (central line), interquartile range (IQR; box) and whiskers extending to 1.5 × the IQR. Boxplots are displayed only for diagnostic groups with ten or more participants. Specific P values can be found in Supplementary Table 3. $^*P < 0.05$, $^{**}P < 0.01$, $^{***}P < 0.001$.
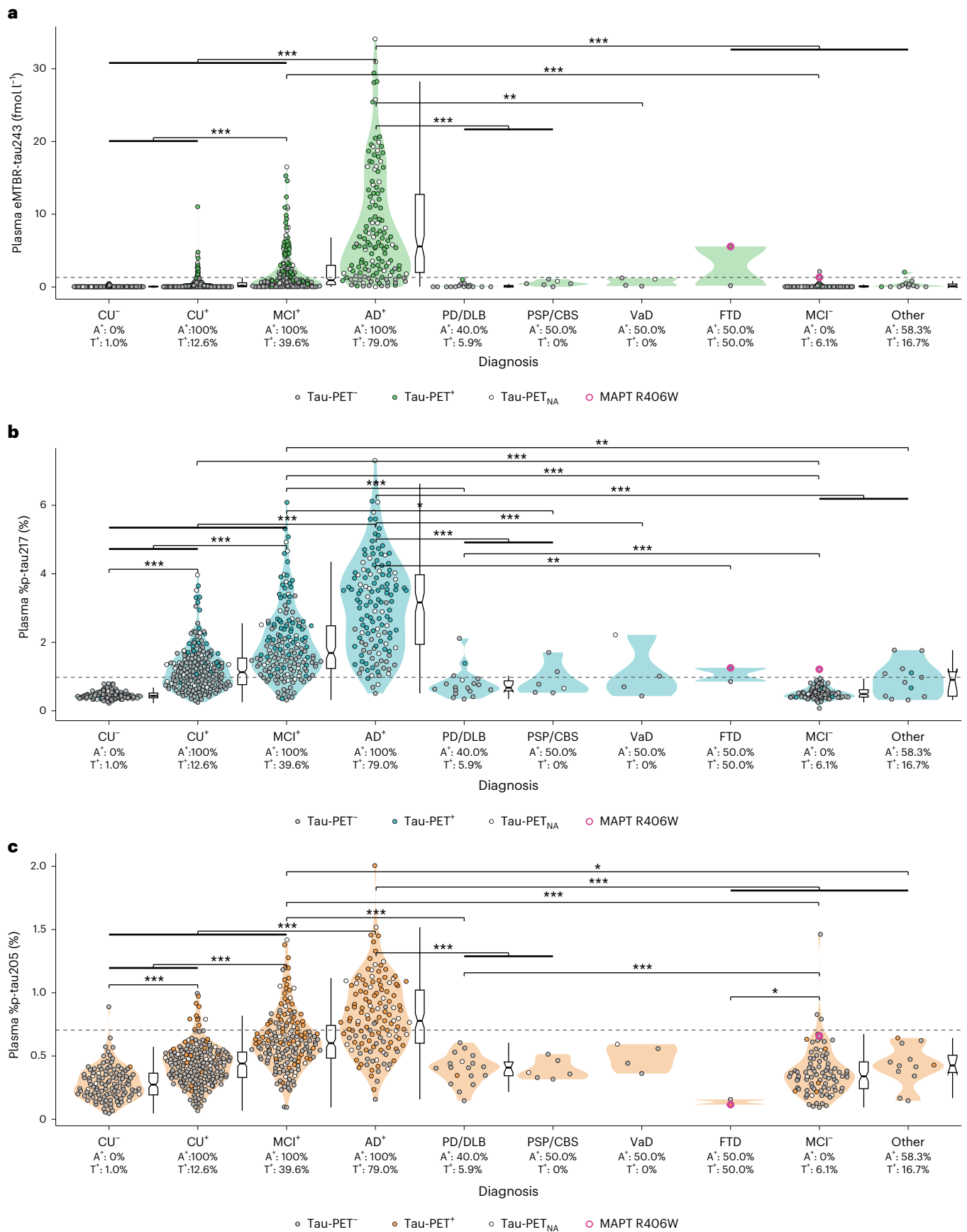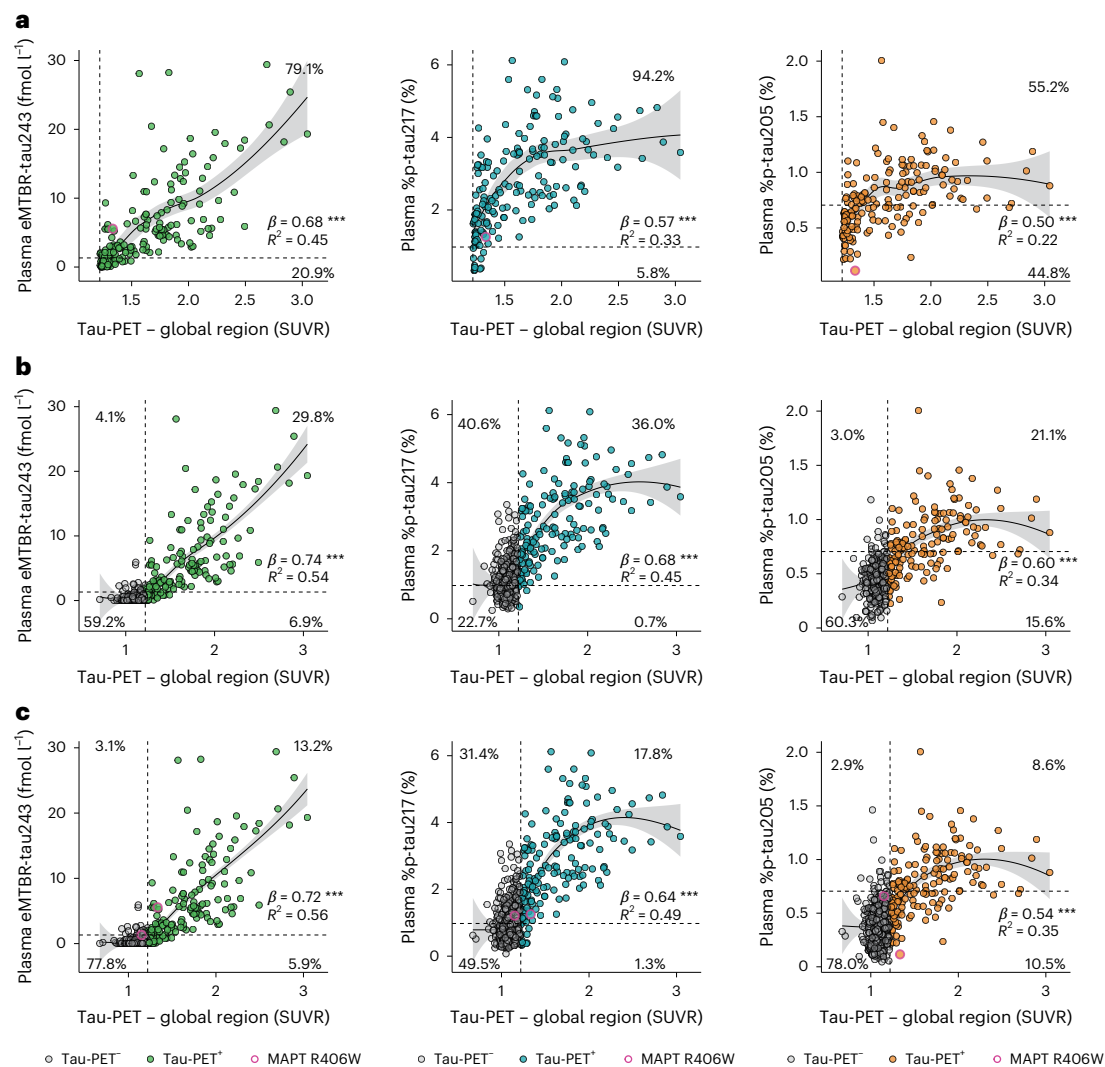
Fig. 2 | Association of plasma tau biomarkers with tau-PET in the validation cohort. a–c, Plots including only tau-PET-positive individuals (**a**, n = 172), Aβ-positive individuals (**b**, n = 436) and all participants (**c**, n = 649). Plasma thresholds were derived using Gaussian mixture modeling. We used previously validated cutoffs for global tau-PET (SUVR > 1.22). Dots are gray color coded to indicate the global tau-PET negativity whereas other color-coded dots indicate tau-PET positivity. MAPT R406W mutation carriers are shown in pink outline. The percentage of individuals in each of the four quadrants is displayed. Standardized β values from linear regression analyses, adjusted for age and sex, are also shown. Locally estimated scatterplot smoothing trend lines (solid black) with 95% CIs (shaded area) illustrate data tendencies. All tests were two sided. All P values were <0.001. ***P < 0.001.

eMTBR-tau243 not only has a stronger association with tau-PET measures compared with %p-tau217, but also provides independent information about insoluble tau pathology that %p-tau217 does not capture.

Associations with Aβ-PET in the validation cohort

In all participants, plasma %p-tau217 demonstrated the strongest association with Aβ-PET (β = 0.81 (95% CI = 0.76–0.87), P < 0.001, R^2 = 0.67). Plasma eMTBR-tau243 also showed a significant association (β = 0.63 (95% CI = 0.56–0.71), P < 0.001, R^2 = 0.39, P_{diff} < 0.001), as well as %p-tau205 (β = 0.48 (95% CI = 0.40–0.56), P < 0.001, R^2 = 0.28, P_{diff} < 0.001; Extended Data Fig. 6a and Supplementary Table 4). Similar findings were observed when focusing on Aβ-positive individuals (Extended Data Fig. 6b and Supplementary Table 4).

When plasma and PET biomarkers were dichotomized into normal and abnormal categories, most participants were Aβ-PET positive but plasma eMTBR-tau243 negative (43.5%) or negative for both biomarkers (40.4%). A smaller proportion was positive for both biomarkers (15.5%), with only 0.6% being plasma positive and PET negative (Extended Data Fig. 3b). Similar trends were observed with plasma %p-tau205, probably

as a result of its higher cutoff, which was influenced by the wide variability in this biomarker. In contrast, plasma %p-tau217 showed higher concordance with Aβ-PET. Most individuals were negative for both biomarkers (39.8%) or positive for both (48.0%), with a smaller proportion being Aβ-PET positive but plasma negative. When all three plasma biomarkers were included in a multivariate model to predict continuous Aβ-PET, plasma %p-tau217 had the highest correlation (β = 0.67 (95% CI = 0.55–0.79), P < 0.001). By comparison, %p-tau205 (β = −0.05 (95% CI = −0.16 to 0.05), P = 0.328) and eMTBR-tau243 (β = 0.08 (95% CI = −0.03 to 0.20), P = 0.162) showed no significant associations in Aβ-positive individuals (Extended Data Fig. 7 and Supplementary Table 5). These results were consistent across all participants. These findings suggest that plasma %p-tau217 provides the strongest association with Aβ-PET of these tau measures and independent information about Aβ pathology that the other tau measures do not capture.

Plasma biomarkers to identify tau- and Aβ-PET outcomes

The accuracy of each plasma biomarker in predicting abnormal tau- and Aβ-PET status was evaluated using receiver operating characteristic
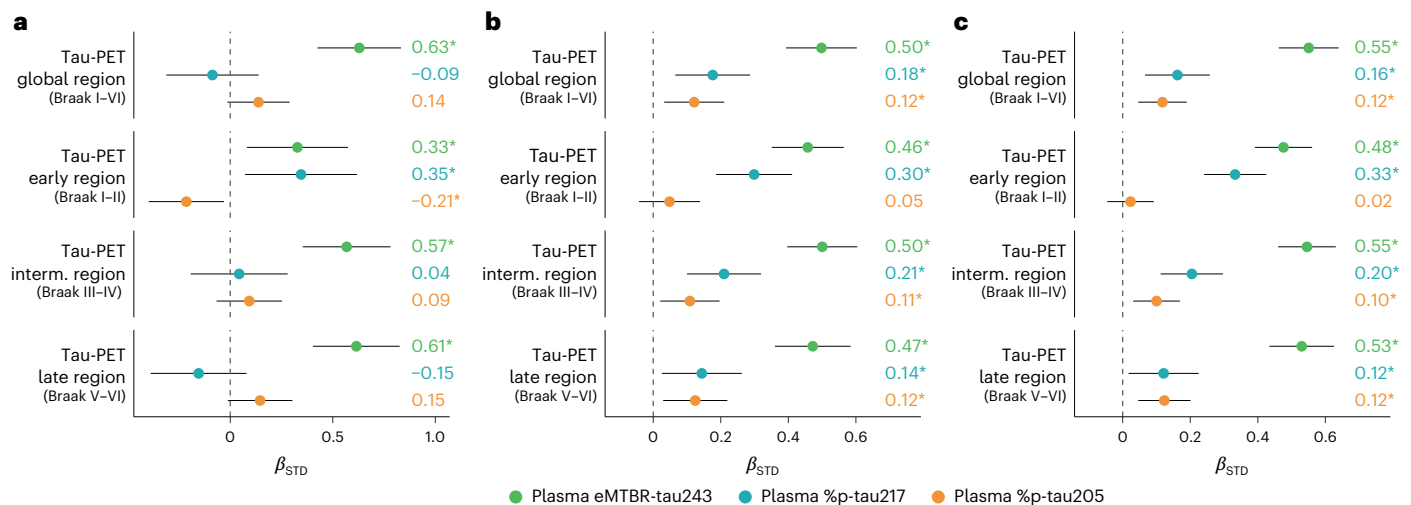
Fig. 3 | Relative associations of plasma biomarkers with continuous tau-PET measures in the validation cohort demonstrate most of the differences in tau-PET that are attributed to plasma eMTBR-tau243. Forest plots display standardized β (colored dots) (β_{STD}), representing effect size to compare the relative importance of each biomarker, along with 95% CIs (black lines) from a multivariate model including all three plasma biomarkers as predictors. **a**–**c**, Analyses shown for tau-PET-positive individuals (**a**, $n = 172$), Aβ-positive individuals (**b**, $n = 436$) and all participants (**c**, $n = 649$). Outcomes are listed on the left. Models also included age and sex as covariates. Vertical dashed lines show 0. Asterisks represent significant effect ($P < 0.05$) for each biomarker and model. Aβ status was assessed using CSF Aβ42/40 or Aβ-PET and tau status using global tau-PET (SUVR > 1.22). All tests were two sided. Specific P values can be found in Supplementary Table 5. interm., intermediate.

(ROC) curves. Among Aβ-positive participants, plasma eMTBR-tau243 consistently demonstrated a significantly higher area under curve (AUC) compared with %p-tau217 and %p-tau205 across all studied tau-PET regions, except for the early tau accumulation region versus %p-tau217. For the global region (Braak I–VI), eMTBR-tau243 had an AUC of 0.92 (95% CI = 0.88–0.96) versus 0.86 for %p-tau217 (95% CI = 0.82–0.91, $P_{diff} = 0.002$) and 0.83 for %p-tau205 (95% CI = 0.78–0.89, $P_{diff} < 0.001$). In the intermediate region (Braak III–IV), the AUC for eMTBR-tau243 was 0.93 (95% CI = 0.90–0.96) versus 0.89 for %p-tau217 (95% CI = 0.86–0.93, $P_{diff} = 0.046$) and 0.85 for %p-tau205 (95% CI = 0.80–0.89, $P_{diff} < 0.001$). Similarly, in the late region (Braak V–VI), eMTBR-tau243 achieved an AUC of 0.95 (95% CI = 0.92–0.97) compared with 0.88 for %p-tau217 (95% CI = 0.83–0.93, $P_{diff} = 0.001$) and 0.88 for %p-tau205 (95% CI = 0.82–0.93, $P_{diff} = 0.004$). For the early region (Braak I–II), however, eMTBR-tau243 had an AUC of 0.87 (95% CI = 0.83–0.91) versus 0.75 for %p-tau205 (95% CI = 0.70–0.80, $P_{diff} < 0.001$), whereas %p-tau217 showed an AUC of 0.83 (95% CI = 0.79–0.88, $P_{diff} = 0.080$) which was not significantly different from that of eMTBR-tau243 (Fig. 4 and Supplementary Table 6).

When analyzing all participants regardless of Aβ status, eMTBR-tau243 still exhibited the highest AUCs for predicting tau-PET status across all studied regions. However, comparing with %p-tau217, the differences were only statistically significant in the global region (eMTBR-tau243: AUC = 0.92 (95% CI = 0.88–0.96) versus %p-tau217: AUC = 0.88 (95% CI = 0.84–0.93), $P_{diff} = 0.008$) and late region (eMTBR-tau243: AUC = 0.94 (95% CI = 0.91–0.98) versus %p-tau217: AUC = 0.89 (95% CI = 0.84–0.95), $P_{diff} < 0.001$). In contrast, plasma %p-tau217 (AUC = 0.97 (95% CI = 0.95–0.98)) outperformed eMTBR-tau243 (AUC = 0.80 (95% CI = 0.76–0.83), $P_{diff} < 0.001$) in predicting Aβ-PET positivity across all participants.

Associations with brain atrophy and cognition

The associations between the plasma biomarkers and downstream effects of AD pathology such as brain atrophy and cognitive impairment were analyzed with a specific focus on the AD spectrum (that is, Aβ-positive individuals). When analyzed individually, plasma eMTBR-tau243 demonstrated the strongest association with brain atrophy measured by MRI ($\beta = 0.46$ (95% CI = 0.38–0.54), $P < 0.001$,

$R^2 = 0.29$), outperforming %p-tau217 ($\beta = 0.40$ (95% CI = 0.31–0.48), $P < 0.001$, $R^2 = 0.24$, $P_{diff} = 0.028$) and %p-tau205 ($\beta = 0.37$ (95% CI = 0.28–0.45), $P < 0.001$, $R^2 = 0.21$, $P_{diff} = 0.006$; Extended Data Fig. 8 and Supplementary Table 7). Similarly, plasma eMTBR-tau243 showed the strongest association with early cognitive impairment as measured by the modified Preclinical Alzheimer Cognitive Composite (mPACC)[21] ($\beta = 0.60$ (95% CI = 0.53–0.68), $P < 0.001$, $R^2 = 0.38$; %p-tau217: $\beta = 0.51$ (95% CI = 0.43–0.60), $P < 0.001$, $R^2 = 0.28$, $P_{diff} = 0.034$; and %p-tau205: $\beta = 0.48$ (95% CI = 0.40–0.57), $P < 0.001$, $R^2 = 0.26$, $P_{diff} = 0.008$). Plasma eMTBR-tau243 also demonstrated the strongest associations with global cognitive performance as assessed by the Mini-Mental State Examination (MMSE)[22] ($\beta = 0.59$ (95% CI = 0.51–0.66), $P < 0.001$, $R^2 = 0.36$; %p-tau217: $\beta = 0.51$ (95% CI = 0.43–0.59), $P < 0.001$, $R^2 = 0.28$, $P_{diff} = 0.012$; and %p-tau205: $\beta = 0.48$ (95% CI = 0.40–0.56), $P < 0.001$, $R^2 = 0.26$, $P_{diff} = 0.002$). In tau-PET-positive individuals, plasma eMTBR-tau243 exhibited the strongest correlations with brain atrophy and cognitive performance. These correlations were significantly higher than those for %p-tau217 and %p-tau205, except for the MMSE where the difference remained significant for %p-tau205 ($P_{diff} = 0.004$), but only approached significance for %p-tau217 ($P_{diff} = 0.052$) (Extended Data Fig. 9 and Supplementary Table 7).

When the three plasma biomarkers were included in multivariate models to examine their independent contributions, plasma eMTBR-tau243 was the strongest predictor of brain atrophy among Aβ-positive participants (eMTBR-tau243: $\beta = 0.37$ (95% CI = 0.23–0.51), $P < 0.001$; %p-tau217: $\beta = 0.03$ (95% CI = −0.11 to 0.18), $P = 0.669$; and %p-tau205: $\beta = 0.10$ (95% CI = 0.02–0.22), $P = 0.099$; Fig. 5 and Supplementary Table 8). The eMTBR-tau243 also had the strongest associations with early cognitive impairment on the mPACC (eMTBR-tau243: $\beta = 0.47$ (95% CI = 0.34–0.59), $P < 0.001$; %p-tau217: $\beta = 0.03$ (95% CI = −0.10 to 0.16), $P = 0.632$; and %p-tau205: $\beta = 0.14$ (95% CI = 0.03–0.25), $P = 0.010$) and also with global cognitive impairment on the MMSE (eMTBR-tau243: $\beta = 0.44$ (95% CI = 0.32–0.57), $P < 0.001$; %p-tau217: $\beta = 0.03$ (95% CI = −0.11 to 0.16), $P = 0.687$; and %p-tau205: $\beta = 0.16$ (95% CI = 0.05–0.26), $P = 0.004$). Plasma %p-tau217 showed no significant independent association with brain atrophy or cognition in the multivariate models, whereas %p-tau205 provided a minor yet significant contribution to predicting brain atrophy and
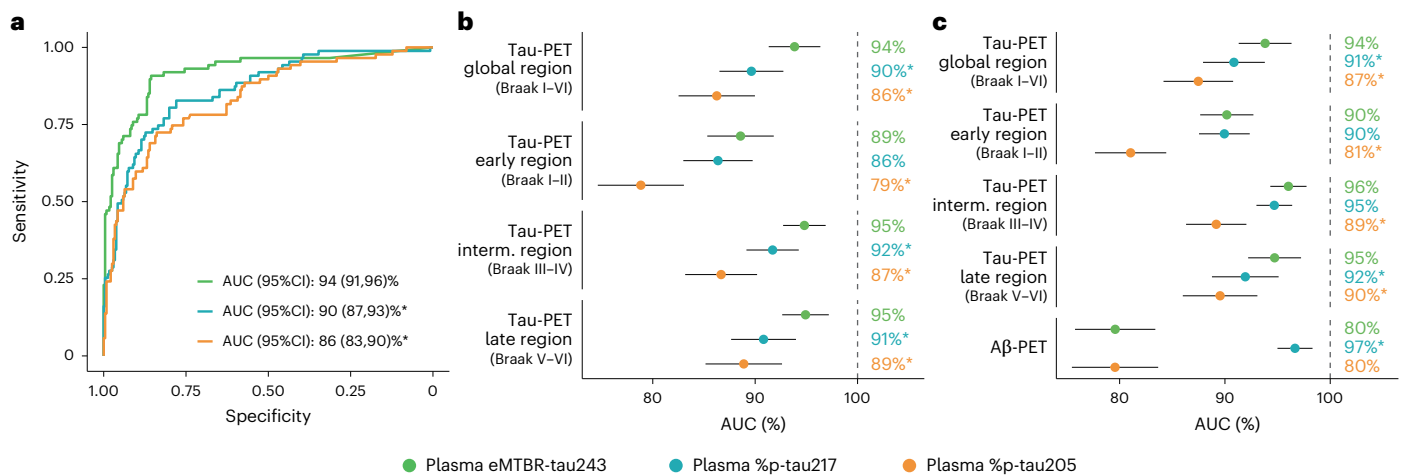
Fig. 4 | Accuracy of assessing Aβ and tau-PET status by region in the validation cohort demonstrates superior performance of plasma eMTBR-tau243 over %p-tau217 and %p-tau205. a, ROC curves for the three plasma biomarkers to assess tau-PET status in Aβ-positive individuals (*n* = 436). AUCs are included in the figure and asterisks represent significantly different AUCs from that of plasma eMTBR-tau243. **b**, AUCs (dots) and 95% CIs (black lines) for all PET status outcomes (listed on the left) shown for each plasma biomarker (color coded) in Aβ-positive individuals (*n* = 436). **c**, The same analysis presented for all participants (*n* = 649 for tau-PET and *n* = 483 for Aβ-PET). Asterisks represent significantly different (*P* < 0.05) AUCs from that of plasma eMTBR-tau243, assessed using the DeLong test. All tests were two sided. Specific *P* values can be found in Supplementary Table 6.

Discussion

In the present study, we developed a new blood biomarker, plasma eMTBR-tau243, that is more strongly associated with, and more specific to, the tau tangle pathology of AD than other established AD plasma biomarkers including %p-tau217. Furthermore, plasma eMTBR-tau243 had a significantly stronger correlation with brain atrophy and cognitive measures than %p-tau217 and %p-tau205, which indicates its potential utility for stage of clinical diagnosis and clinical trials. For example, plasma eMTBR-tau243 could potentially serve as an alternative to tau-PET for monitoring tau pathology in clinical trials and could improve diagnostic and prognostic accuracy in clinical practice.

Plasma eMTBR-tau243, which has a cleavage at the C-terminal side of residue 256 (valine), was strongly associated with AD tau tangle pathology and AD symptoms. The CSF assay for MTBR-tau243 using a tryptic peptide did not show this association, potentially as a result of a larger contribution of non-CNS tau species derived from peripheral tissues in the plasma than in the CSF when using the tryptic MTBR-tau243 peptide[19]. We have previously shown that the early R1 region (surrounding residues 243–254) was significantly enriched in brains with more advanced AD, whereas the late R1 region (surrounding residues 260–267) was not[23]. A recent cryo-electron microscopy (cryo-EM) study using various lengths of recombinant tau with different truncation sites also indicated that tau species containing mid-domain (residues 151, 181 and 231) and early R1 regions (residue 244) either did not form filament structures or formed structures that were not similar to AD paired helical filaments (PHFs)[24]. Importantly, this cryo-EM study revealed that the high tau aggregation competency to form the AD PHF structure was observed once the truncation occurred in the late R1 region (around residue 258), which could lead to shedding of the eMTBR-tau243 fragment peptide from the insoluble tau aggregates to soluble compartments including biofluid. These results suggest that the specific endogenous cleavage in the R1 region (around residue 258) may precede or contribute to AD PHF formation, which is consistent with our findings that the eMTBR-tau243 ending at residue 256 reflects AD tangle pathology specifically. In addition, we found that deamidation at asparagine residue 255 identified plasma eMTBR-tau243 that

was associated with AD tau pathology. Deamidation is one of the most common post-translational modifications, typically increases with time and is irreversible under physiological conditions[25]. We speculate that deamidation occurs more frequently to tau species that have been sequestered in AD brain aggregates over months to years, which might distinguish them from peripheral tau and other more newly formed tau species.

Next, we compared the relationships of plasma eMTBR-tau243 and two phosphorylated tau measures (%p-tau217 and %p-tau205) with AD clinical stages, AD pathologies measured by tau- and Aβ-PET, brain atrophy measured by MRI and cognitive performance as assessed by mPACC and MMSE. Plasma MTBR-tau243 was significantly increased in Aβ-positive MCI and further increased in AD dementia (up to 200-fold) compared with CU, but not in Aβ-positive CU compared with Aβ-negative CU, indicating that elevated plasma eMTBR-tau243 levels were not directly attributable to Aβ pathology. This was in contrast with plasma p-tau measures, including %p-tau217, that are more associated with Aβ-PET[14,18] or with Aβ pathology in postmortem studies[15]. Indeed, %p-tau217 and %p-tau205 significantly increased in Aβ-positive CU compared with Aβ-negative CU and demonstrated the different trajectories over the disease continuum compared with eMTBR-tau243. In addition, we observed that plasma eMTBR-tau243 levels were not increased in other dementia syndromes (including PSP, CBS and FTD) that are often associated with primary 3R or 4R tauopathies, suggesting a specificity for AD-related tau pathology. Notably, we found that eMTBR-tau243 was particularly increased in one of two MAPT R406W mutation carriers that was Aβ negative but had a positive tau-PET status, whereas eMTBR-tau243 was not increased in the tau-PET-negative mutation carrier. Tau pathology in the MAPT R406W mutation carriers is known to be similar to AD tau pathology, including the filament structure elucidated by immunohistochemistry[26,27] and cryo-EM[28] and reactive to the multiple AD tau-PET tracers[29–34], supporting our finding that eMTBR-tau243 is a specific biomarker for AD-like tau tangles and not for Aβ plaques.

Plasma eMTBR-tau243 demonstrated the highest and most linear correlation with tau-PET. This was observed in the entire cohort, and also in the Aβ-positive group, especially in tau-PET-positive individuals. This suggests that eMTBR-tau243 is a biomarker that specifically reflects aggregated tau pathology independent of Aβ pathology. Although %p-tau217 and %p-tau205 were also well correlated with
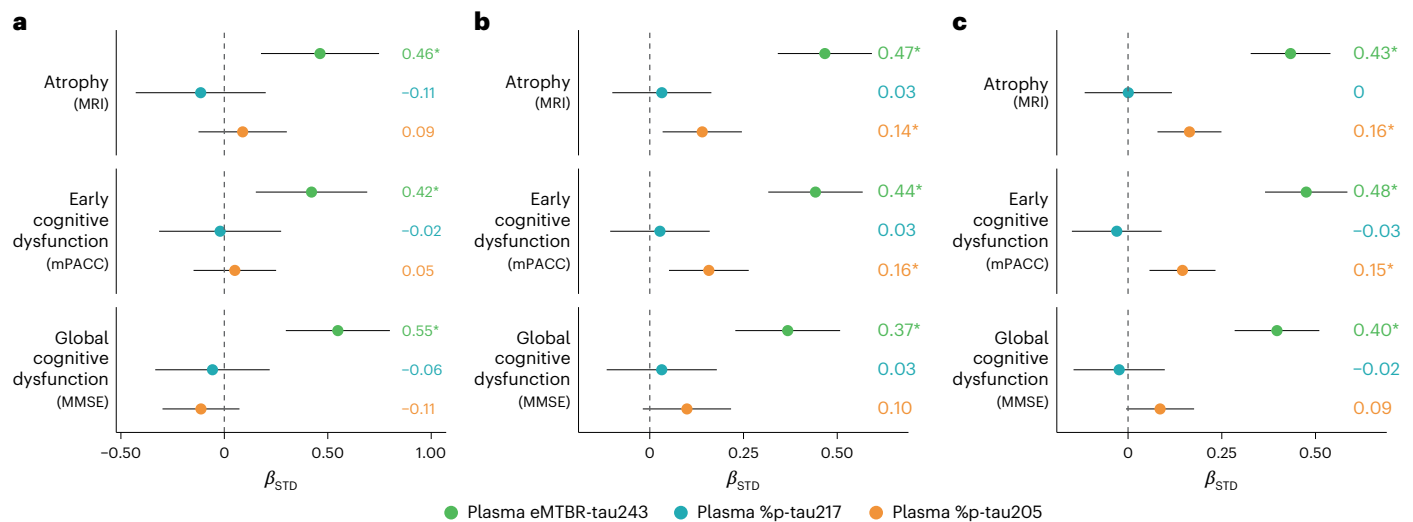
early cognitive performance. Detailed results, including analyses for all participants and tau-positive individuals, are shown in Fig. 5 and Supplementary Table 8.

Fig. 5 | Relative associations of plasma biomarkers and brain atrophy and cognition in the validation cohort. Forest plots represent standardized β (colored dots) (β_{STD}) and 95% CI (black lines) from a multivariate model including all three plasma biomarkers as predictors. **a–c**, Analysis shown for tau-PET-positive individuals (**a**, cortical thickness: $n = 159$; early cognitive dysfunction: $n = 143$; global cognitive dysfunction: $n = 160$), Aβ-positive individuals (**b**, cortical thickness: $n = 413$; early cognitive dysfunction: $n = 445$; global cognitive dysfunction: $n = 481$) and all participants (**c**, cortical thickness: $n = 522$; early cognitive dysfunction: $n = 556$; global cognitive dysfunction: $n = 593$). Outcomes are listed on the left. Models were adjusted for age and sex (and education for cognitive outcomes). Vertical dashed lines indicate 0. Asterisks represent significant effect ($P < 0.05$) for each biomarker and model. Aβ status was assessed using CSF Aβ42/40 or Aβ-PET and tau status using global tau-PET (SUVR > 1.22). All tests were two sided.

tau-PET, they had a substantial increase in the p-tau measures before the tau-PET measure increased and a nonlinear logarithmic relationship with tau-PET that plateaued after exceeding the tau-PET threshold. This suggests that the plasma p-tau biomarkers studied here may be associated with tau pathology as a result of their quantitative relationship with the amount of Aβ pathology, as observed in the previous study of CSF MTBR-tau243 (ref. 19). In addition, multivariate modeling analysis with all three plasma tau measures as predictors of tau- or Aβ-PET indicated that eMTBR-tau243 has the largest independent association with tau-PET and may uniquely recapitulate the mature tau tangle pathology that occurs in the symptomatic AD pathological continuum which p-tau measures do not reflect. In contrast, plasma %p-tau217 showed the strongest independent association with Aβ-PET in a multivariate model that predicted continuous Aβ-PET burden, corroborating previous findings that identified %p-tau217 as the most accurate biomarker to identify early AD pathological changes[12,35]. Finally, we found that, among the three plasma biomarkers, eMTBR-tau243 (in both univariate and multivariate models) showed the strongest associations with cognitive and neurodegenerative measures, suggesting that eMTBR-tau243 is a superior plasma biomarker for predicting downstream phenotypic changes in AD.

Notably, plasma eMTBR-tau243 in Aβ-positive participants exhibited significantly higher and more linear correlations with tau-PET signal in intermediate (Braak III–IV) and late (Braak V–VI) tau-accumulating regions compared with the p-tau species. In contrast, the associations with tau-PET signal in early tau-accumulating regions (Braak I–II) did not differ between eMTBR-tau243 and %p-tau217, which implies that plasma eMTBR-tau243 better recapitulates more advanced tau pathological stages (that is, neocortical spreading phase) compared with the early pathological stages (for example, entorhinal accumulation phase).

Study limitations include the relatively large volume of plasma (1.5 ml) required for accurate measurement in this first version of the assay. This new plasma biomarker should also be further validated in larger and even more real-world populations, including cohorts with a higher frequency of other neurodegenerative or psychiatric diseases, medical comorbidities and other demographic backgrounds (for example, racial and ethnic differences) that may affect plasma biomarker measurements.

In conclusion, our findings indicate that plasma eMTBR-tau243 reflects aggregated tau AD-related proteinopathy that steadily increases during the clinical symptomatic phase of AD and may be used to stage AD tauopathy. This measure could help determine whether cognitive decline is caused by AD pathology from tau tangles in individual patients with cognitive symptoms. It may also be useful in clinical practice to help identify those symptomatic AD patients with lower levels of tau who are more likely to benefit from anti-Aβ immunotherapies[2]. Although tau-PET is still useful as the gold standard for tau pathology and provides regional information (not possible with blood biomarkers), plasma eMTBR-tau243 might be a viable alternative to tau-PET for identifying suitable study participants in clinical trials and, even more importantly, it might be used as an important study endpoint to cost-effectively determine whether a new therapy affects insoluble tau proteinopathy in the brain. Furthermore, CSF MTBR-tau243 was recently adopted as the fluid biomarker representing insoluble tau aggregate pathology (T_2) by commonly used A/T/(N) (amyloid/tau/(neurodegeneration)) criteria for AD[19,36,37]. Our findings suggest that plasma eMTBR-tau243 may also be considered as a 'T_2 (AD tau proteinopathy)' biomarker for diagnosis and staging of AD.

Online content

Any methods, additional references, Nature Portfolio reporting summaries, source data, extended data, supplementary information, acknowledgements, peer review information; details of author contributions and competing interests; and statements of data and code availability are available at https://doi.org/10.1038/s41591-025-03617-7.

References

1. van Dyck, C. H. et al. Lecanemab in early Alzheimer's disease. *N. Engl. J. Med.* https://doi.org/10.1056/NEJMoa2212948 (2022).
2. Sims, J. R. et al. Donanemab in early symptomatic Alzheimer disease: the TRAILBLAZER-ALZ 2 randomized clinical trial. *JAMA* **330**, 512–527 (2023).
3. Price, J. L. & Morris, J. C. Tangles and plaques in nondemented aging and 'preclinical' Alzheimer's disease. *Ann. Neurol.* **45**, 358–368 (1999).

4. Ossenkoppele, R., van der Kant, R. & Hansson, O. Tau biomarkers in Alzheimer's disease: towards implementation in clinical practice and trials. *Lancet Neurol.* **21**, 726–734 (2022).

5. Ossenkoppele, R. et al. Amyloid and tau PET-positive cognitively unimpaired individuals are at high risk for future cognitive decline. *Nat. Med.* **28**, 2381–2387 (2022).

6. Smith, R., Wibom, M., Pawlik, D., Englund, E. & Hansson, O. Correlation of in vivo [¹⁸F]flortaucipir with postmortem Alzheimer disease tau pathology. *JAMA Neurol.* **76**, 310–317 (2019).

7. Lowe, V. J. et al. Tau-positron emission tomography correlates with neuropathology findings. *Alzheimers Dement.* **16**, 561–571 (2020).

8. Hansson, O. Biomarkers for neurodegenerative diseases. *Nat. Med.* **27**, 954–963 (2021).

9. Smith, R. et al. Tau-PET is superior to phospho-tau when predicting cognitive decline in symptomatic AD patients. *Alzheimer's Dement.* **19**, 2497–2507 (2023).

10. Janelidze, S. et al. Plasma P-tau181 in Alzheimer's disease: relationship to other biomarkers, differential diagnosis, neuropathology and longitudinal progression to Alzheimer's dementia. *Nat. Med.* **26**, 379–386 (2020).

11. Palmqvist, S. et al. Discriminative accuracy of plasma phospho-tau217 for Alzheimer disease vs other neurodegenerative disorders. *JAMA* **324**, 772–781 (2020).

12. Barthélemy, N. R. et al. Highly accurate blood test for Alzheimer's disease is similar or superior to clinical cerebrospinal fluid tests. *Nat. Med.* **30**, 1085–1095 (2024).

13. Hansson, O., Blennow, K., Zetterberg, H. & Dage, J. Blood biomarkers for Alzheimer's disease in clinical practice and trials. *Nat. Aging* **3**, 506–519 (2023).

14. Therriault, J. et al. Association of phosphorylated tau biomarkers with amyloid positron emission tomography vs tau positron emission tomography. *JAMA Neurol.* **80**, 188–199 (2023).

15. Salvadó, G. et al. Specific associations between plasma biomarkers and postmortem amyloid plaque and tau tangle loads. *EMBO Mol. Med.* **15**, e2463 (2023).

16. Meeker, K. L. et al. Comparison of cerebrospinal fluid, plasma and neuroimaging biomarker utility in Alzheimer's disease. *Brain Commun.* **6**, fcae081 (2024).

17. Barthélemy, N. R. et al. A soluble phosphorylated tau signature links tau, amyloid and the evolution of stages of dominantly inherited Alzheimer's disease. *Nat. Med.* **26**, 398–407 (2020).

18. Mattsson-Carlgren, N. et al. Aβ deposition is associated with increases in soluble and phosphorylated tau that precede a positive Tau PET in Alzheimer's disease. *Sci. Adv.* **6**, eaaz2387 (2020).

19. Horie, K. et al. CSF MTBR-tau243 is a specific biomarker of tau tangle pathology in Alzheimer's disease. *Nat. Med.* **29**, 1954–1963 (2023).

20. Barthélemy, N. R. et al. CSF tau phosphorylation occupancies at T217 and T205 represent improved biomarkers of amyloid and tau pathology in Alzheimer's disease. *Nat. Aging* **3**, 391–401 (2023).

21. Donohue, M. C. et al. The preclinical Alzheimer cognitive composite: measuring amyloid-related decline. *JAMA Neurol.* **71**, 961–970 (2014).

22. Folstein, M. F., Folstein, S. E. & McHugh, P. R. 'Mini-mental state': a practical method for grading the cognitive state of patients for the clinician. *J. Psychiatric Res.* **12**, 189–198 (1975).

23. Horie, K., Barthélemy, N. R., Sato, C. & Bateman, R. J. CSF tau microtubule binding region identifies tau tangle and clinical stages of Alzheimer's disease. *Brain* **144**, 515–527 (2021).

24. Lövestam, S. et al. Assembly of recombinant tau into filaments identical to those of Alzheimer's disease and chronic traumatic encephalopathy. *eLife* **11**, e76494 (2022).

25. Robinson, N. E. & Robinson, A. B. Molecular clocks. *Proc. Natl Acad. Sci. USA* **98**, 944–949 (2001).

26. Lindquist, S. G. et al. Alzheimer disease-like clinical phenotype in a family with FTDP-17 caused by a MAPT R406W mutation. *Eur. J. Neurol.* **15**, 377–385 (2008).

27. de Silva, R. et al. An immunohistochemical study of cases of sporadic and inherited frontotemporal lobar degeneration using 3R- and 4R-specific tau monoclonal antibodies. *Acta Neuropathol.* **111**, 329–340 (2006).

28. Qi, C. et al. Tau filaments with the Alzheimer fold in human MAPT mutants V337M and R406W. *Nat. Struct. Mol. Biol.* https://doi.org/10.1038/s41594-025-01498-5 (2025).

29. Smith, R. et al. ¹⁸F-AV-1451 tau PET imaging correlates strongly with tau neuropathology in MAPT mutation carriers. *Brain* **139**, 2372–2379 (2016).

30. Wolters, E. E. et al. [¹⁸F]Flortaucipir PET across various MAPT mutations in presymptomatic and symptomatic carriers. *Neurology* **97**, e1017–e1030 (2021).

31. Tsai, R. M. et al. ¹⁸F-flortaucipir (AV-1451) tau PET in frontotemporal dementia syndromes. *Alzheimer's Res. Ther.* **11**, 13 (2019).

32. Jones, D. T. et al. In vivo ¹⁸F-AV-1451 tau PET signal in MAPT mutation carriers varies by expected tau isoforms. *Neurology* **90**, e947–e954 (2018).

33. Levy, J. P. et al. ¹⁸F-MK-6240 tau-PET in genetic frontotemporal dementia. *Brain* **145**, 1763–1772 (2021).

34. Santillo, A. F. et al. [¹⁸F]RO948 tau positron emission tomography in genetic and sporadic frontotemporal dementia syndromes. *Eur. J. Nucl. Med. Mol. Imaging* **50**, 1371–1383 (2023).

35. Palmqvist, S. et al. Blood biomarkers to detect Alzheimer disease in primary c775are and secondary care. *JAMA* **332**, 1245–1257 (2024).

36. Jack, C. R. et al. A/T/N: an unbiased descriptive classification scheme for Alzheimer disease biomarkers. *Neurology* **87**, 539–547 (2016).

37. Jack, C. R. Jr. et al. Revised criteria for diagnosis and staging of Alzheimer's disease: Alzheimer's Association Workgroup. *Alzheimer's Dement.* **20**, 5143–5169 (2024).

[1]The Tracy Family SILQ Center, Washington University School of Medicine, St. Louis, MO, USA. [2]Department of Neurology, Washington University School of Medicine, St. Louis, MO, USA. [3]Eisai Inc., Nutley, NJ, USA. [4]Clinical Memory Research Unit, Department of Clinical Sciences Malmö, Lund University, Lund, Sweden. [5]Department of Psychiatry, Washington University School of Medicine, St. Louis, MO, USA. [6]Department of Radiology, Washington University School of Medicine, St. Louis, MO, USA. [7]Charles F. and Joanne Knight Alzheimer Disease Research Center, Washington University School of Medicine, St. Louis, MO, USA. [8]Hope Center for Neurological Disorders, Washington University School of Medicine, St. Louis, MO, USA. [9]Memory Clinic, Skåne University Hospital, Malmö, Sweden. [10]Wallenberg Center for Molecular Medicine, Lund University, Lund, Sweden. [11]Alzheimer Center Amsterdam, Neurology, Vrije Universiteit Amsterdam, Amsterdam UMC, location VUmc, Amsterdam, The Netherlands. [12]Amsterdam Neuroscience, Neurodegeneration, Amsterdam, The Netherlands. [13]These authors contributed equally: Kanta Horie, Gemma Salvadó, Oskar Hansson, Randall J. Bateman. [14]These authors jointly supervised this work: Oskar Hansson, Randall J. Bateman. ✉e-mail: horiekanta@wustl.edu; oskar.hansson@med.lu.se; batemanr@wustl.edu

Methods

Participants

Participants were included from the Swedish BioFINDER-2 study (NCT03174938)[11] at Lund University (Lund, Sweden), and the Knight ADRC study at Washington University (St. Louis, MO, USA). The BioFINDER-2 study participants were recruited at Skåne University Hospital and the Hospital of Ängelholm in Sweden. Details on recruitment, exclusion and inclusion criteria have been presented before[11]. The Knight ADRC study consisted of community-dwelling volunteers enrolled in studies of memory and aging at Washington University. Fluid samples were collected in the Aβ-stable isotope-labeling, kinetics study[38] participants. introduced from the study of memory and aging in the Knight ADRC.

In the present study, we analyzed three different cohorts. In the pilot BioFINDER-2 cohort ($n = 108$), participants were divided into cognitively impaired (CU) either Aβ-negative or -positive (CU⁻ ($n = 57$) or CU⁺ ($n = 4$), respectively), mild cognitive impairment (MCI) Aβ-positive (MCI⁺; $n = 10$) and AD dementia Aβ-positive (AD⁺; $n = 37$). In the pilot Knight ADRC cohort ($n = 55$), participants were divided into CU⁻ ($n = 15$) and CU⁺ ($n = 14$) with Clinical Dementia Rating (CDR) = 0, very mild AD dementia (CDR = 0.5), Aβ-positive ($n = 18$) or AD⁺ with CDR ≥ 1 ($n = 8$). In the BioFINDER-2 validation cohort ($n = 739$), participants were divided into CU⁻ ($n = 110$), CU⁺ ($n = 198$), MCI⁺ ($n = 169$), AD⁺ ($n = 134$), Parkinson's disease or Lewy body dementia (PD or DLB) ($n = 18$), progressive supranuclear palsy or corticobasal syndrome (PSP or CBS) ($n = 6$), vascular dementia (VaD; $n = 4$), frontotemporal dementia (FTD; $n = 2$), R406W MAPT mutation carriers ($n = 2$) (one tau-PET positive and the other tau-PET negative), MCI without Aβ-positive (MCI⁻) ($n = 86$) and other neurodegenerative dementia ($n = 12$).

In accordance with the research framework by the National Institute on Aging–Alzheimer's Association study, individuals with subjective cognitive decline and cognitively healthy controls were considered to be the CU group. All participants gave written informed consent and ethical approval was granted by the Regional Ethical Committee in Lund Sweden and the Washington University Human Research Protection Office, respectively.

Fluid samples for plasma eMTBR-tau243 method development

Three kinds of plasma samples were made by mixing plasma samples from multiple participants (in the Knight ADRC) with low, middle and high tau-PET status, respectively. The corresponding CSF samples were also made.

Plasma measurements

Measurement of plasma eMTBR-tau243 was performed at Washington University using the newly developed immunoprecipitation–MS (IP–MS) method. We developed the new tau purification method with the monoclonal antibody HJ32.11 binding near residue 243 (ref. 19). HJ32.11 antibody was coupled to Sepharose beads at 3 mg g⁻¹ concentration and the beads with 45 μg of HJ32.11 antibody were added into 1.4 ml of plasma clarified by centrifugation (1.5 ml of plasma, originally), followed by the IP and Arg-C (Promega) digestion to recover the tau species with an endogenously cleaved site at residue 256. We quantified the specific tau peptide with deamidation and C-terminal cleavage at residues 255 (asparagine) and 256 (valine) (sequence: LQTAPVPMPDLKD*V, D* is deamidated asparagine) by using the high-resolution MS analysis on an anoAcquity UPLC system (Waters) coupled to an Orbitrap Tribrid Eclipse (Thermo Fisher Scientific) operating in a parallel reaction monitoring mode. AQUA internal standard peptide labeled with [¹³C¹⁵N]lysine was used as the reference standard to quantify the plasma eMTBR-tau243 species. As different lots of internal standard solution were used for the BioFINDER-2 cohort and the Knight ADRC cohort analyses, the absolute levels of plasma eMTBR-tau243 were calculated in different ranges, although the biomarker characteristics could be assessed within each cohort. Interday assay variability (CV) assessed by

quality control plasma samples was <10% in the BioFINDER-2 validation cohort analysis. The schematic procedure of plasma eMTBR-tau243 analysis is described in Supplementary Fig. 3.

Measurement of plasma %p-tau217 and %p-tau205 was performed for the post-IP plasma (after immunodepletion with HJ32.11) at Washington University, using the previously reported method with IP–MS[12]. For %p-tau217, the ratio between signals from TPSLPpTPPPTR 212–221 phosphorylated peptide at T217 and the unmodified peptide was used. For %p-tau205, the ratio between signals from SGYSSPGSPGpTPGSR 195–209 phosphorylated peptide at T205 and unmodified peptide was used.

CSF measurements

Measurement of CSF MTBR-tau243 was performed at Washington University using the previously reported methods with IP–MS, chemical extraction or MS analysis[19,23].

In addition, CSF Aβ42/40 levels were used in both cohorts to assess Aβ positivity. In the BioFINDER-2 cohort, CSF levels of Aβ42/40 were measured as previously explained[11]. A threshold of 0.080, based on a Gaussian mixture model, determined Aβ positivity[39]. In the Knight ADRC cohort, CSF Aβ42/40 levels were measured by MS as explained previously[38]. A threshold of 0.1389, maximizing the combined sensitivity and specificity in distinguishing Aβ-PET status, was used to determine Aβ positivity[23].

Imaging acquisition and quantification

In the BioFINDER-2 cohort, Aβ- and tau-PET-acquiring methods have been previously reported[11]. Briefly, Aβ-PET was acquired using [¹⁸F]flutemetamol and tau-PET using [¹⁸F]RO948. Of note, most of the patients with AD dementia did not undergo amyloid-PET in BioFINDER-2, because of the study design. For tau-PET, standardized uptake value ratios (SUVRs) were calculated using the inferior cerebellum cortex as a reference region and binding from global region of interest (ROI) was used for the main analyses (Braak I–VI). We also quantified tau-PET in early (Braak I–II), intermediate (Braak III–IV) and late (Braak V–VI) regions of tau deposition[40]. Tau positivity was assessed based on tau-PET in all cases. In the Braak I–VI global region, cutoff for positivity was set at SUVR > 1.22 (ref. 41).

We used T1-weighted, anatomical magnetization-prepared, rapid gradient echo (MPRAGE) images (1-mm isotropic voxels) for assessing cortical thickness. A cortical thickness meta-ROI was calculated including entorhinal, inferior temporal, middle temporal and fusiform regions using FreeSurfer (v.6.0, https://surfer.nmr.mgh.harvard.edu) parcellation, which are areas known to be susceptible to AD-related atrophy.

Cognitive tests

MMSE (measure of global cognition) and mPACC (sensitive to early cognitive impairment) were used as a measure of global cognition in the BioFINDER-2 cohort. The mPACC-5 composite was calculated using the mean of z-scores of the AD Assessment Scale (ADAS) delayed recall (weighted double), animal fluency, MMSE and Trail Making Test A[42] as a sensitive measure of early cognitive impairment[21]. We calculated z-scores with a group of CU⁻ individuals as reference.

Statistical analyses

Statistical analyses were conducted using R v.4.1.0. Differences in plasma biomarker levels across diagnostic groups were assessed using ANCOVA, adjusted for age and sex, followed by Tukey's corrected post hoc pairwise comparisons. Spearman's ρ was calculated to evaluate correlations between plasma eMTBR-tau243 and CSF MTBR-tau243, in the pilot cohorts, as well as among plasma biomarkers in the validation cohort.

In the validation cohort, linear regression models were used to investigate associations between plasma biomarkers (outcomes) and tau- and Aβ-PET load (predictors, analyzed in separate models),

adjusting for age and sex. The relative strength of these associations, compared with those involving plasma eMTBR-tau243, was determined by bootstrapping the differences (1,000 resamples). Associations between plasma biomarkers and neurodegeneration (cortical thickness from MRI) and cognitive performance (mPACC and MMSE) were similarly evaluated using linear regression, with plasma biomarkers as predictors and neurodegeneration or cognitive measures as outcomes. Models were adjusted for age and sex, with additional adjustment for years of education in cognitive analyses. To assess the independent predictive value of plasma biomarkers for AD-related outcomes, multivariate linear regression models were performed, including all plasma biomarkers as predictors while adjusting for age and sex (and years of education for cognitive outcomes).

The diagnostic accuracy of plasma biomarkers for differentiating tau- and Aβ-PET-positive or -negative status was evaluated using ROC curves and AUCs, calculated using the pROC package. Comparisons of AUCs between biomarkers were performed using the DeLong test. When applicable, analyses were stratified by tau-PET-positive individuals, Aβ-positive individuals and the full cohort.

All tests were two sided, with statistical significance defined as $P < 0.05$.

Reporting summary

Further information on research design is available in the Nature Portfolio Reporting Summary linked to this article.

Data availability

The datasets generated and/or analyzed during the present study are available from the corresponding authors (K.H., R.J.B. and O.H.). We will share datasets within the restrictions of institutional review board (IRB) ethics approvals, upon reasonable request. Pseudonymized data from the BioFINDER-2 will be shared by request from a qualified academic investigator for the sole purpose of replicating procedures and results presented in the article, as long as data transfer is in agreement with EU legislation on the general data protection regulation and decisions by the Ethical Review Board of Sweden and Region Skåne, which should be regulated in a material transfer agreement. The Knight ADRC data are available to qualified investigators who have a proposal approved by R.J.B. and an institutional committee (https://knightadrc.wustl.edu/Research/ResourceRequest.htm). The study must be approved by an IRB to ensure ethical research practices and investigators must agree to the terms and conditions of the data use agreement, which includes not distributing the data without permission.

References

38. Patterson, B. W. et al. Age and amyloid effects on human central nervous system amyloid-beta kinetics. *Ann. Neurol.* **78**, 439–453 (2015).
39. Pichet Binette, A. et al. Amyloid-associated increases in soluble tau relate to tau aggregation rates and cognitive decline in early Alzheimer's disease. *Nat. Commun.* **13**, 6635 (2022).
40. Cho, H. et al. In vivo cortical spreading pattern of tau and amyloid in the Alzheimer disease spectrum. *Ann. Neurol.* **80**, 247–258 (2016).
41. Leuzy, A. et al. A multicenter comparison of [18F]flortaucipir, [18F]RO948, and [18F]MK6240 tau PET tracers to detect a common target ROI for differential diagnosis. *Eur. J. Nucl. Med. Mol. Imaging* **48**, 2295–2305 (2021).
42. Armitage, S. G. An analysis of certain psychological tests used for the evaluation of brain injury. *Psychol. Monographs* **60**, i–48 (1946).

Acknowledgements

Author contributions

K.H. and R.J.B. conceived the goal to develop a blood plasma biomarker of tau aggregates utilizing MTBR-tau243. K.H., O.H. and R.J.B. conceived the study to assess the relationships with clinical study measures. K.H., R.K.K. and R.J.B. developed the plasma eMTBR-tau243 method. K.H., R.K.K., N.R.B. and Y.H. executed plasma biomarker experiments. G.S. performed statistical analyses. K.H., G.S., S.J., O.H. and R.J.B. analyzed and interpreted the data. H.J. and D.M.H., with R.J.B. and K.H., developed and provided the antibody for tau IP. O.H. provided mentorship, and founded and led the Swedish BioFINDER-2 study that enabled recruitment of participants to the present study. J.C.M. provided mentorship, and founded and led the Knight ADRC that enabled recruitment of participants in the present study. S.J., S.P. and E.S. coordinated sample selection at BioFINDER-2 and provided associated data. S.P. did clinical assessments in BioFINDER-2. R.J.B. founded the Tracy Family SILQ Center, providing resources and goals to develop new biomarkers and mentorship. K.H., G.S. and O.H. wrote the initial draft of the paper. O.H. and

R.J.B. supervised the research study and analyses. All authors made substantial contributions to the subsequent version of the paper and approved the final version for submission.

Additional information

Extended data is available for this paper at https://doi.org/10.1038/s41591-025-03617-7.

Supplementary information The online version contains supplementary material available at https://doi.org/10.1038/s41591-025-03617-7.

Correspondence and requests for materials should be addressed to Kanta Horie, Oskar Hansson or Randall J. Bateman.

Peer review information *Nature Medicine* thanks Thomas Karikari and the other, anonymous, reviewer(s) for their contribution to the peer review of this work. Primary Handling Editor: Jerome Staal, in collaboration with the *Nature Medicine* team.

Reprints and permissions information is available at www.nature.com/reprints.
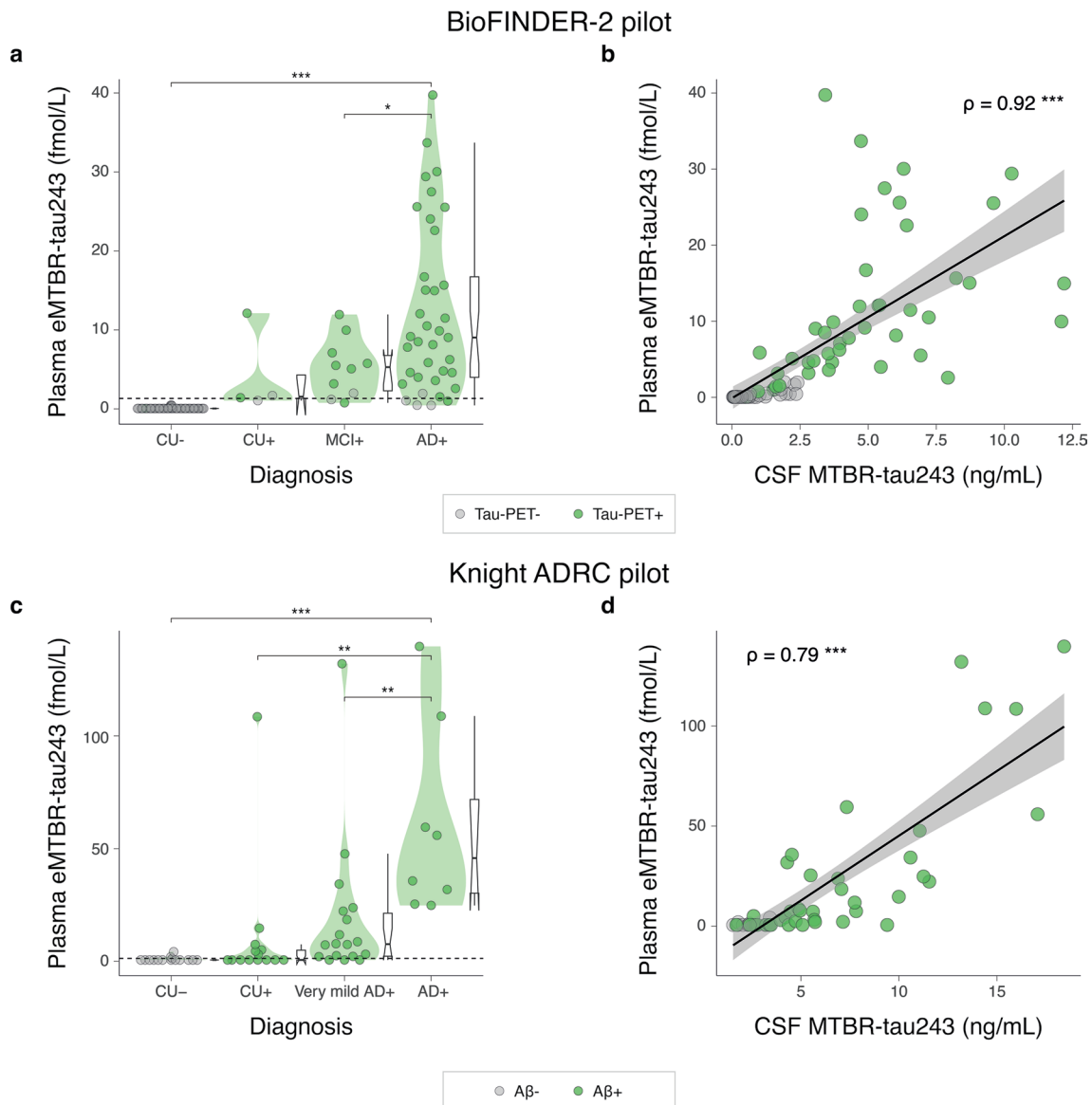
Extended Data Fig. 1 | Plasma eMTBR-tau243 changes by diagnosis and correlations with CSF MTBR-tau243 in the two pilot cohorts. a,c, Levels of plasma eMTBR-tau243 by clinical diagnosis and Aβ status in the pilot BioFINDER-2 cohort (n = 108) (a) and the pilot Knight ADRC cohort (n = 55) (c). Differences in plasma eMTBR-tau243 levels by diagnostic groups were tested using ANOVA and the post hoc analyses were performed two-sided using. Boxplots summarize data distribution, showing the median (central line), interquartile range (box), and whiskers extending to 1.5 times the interquartile range. *, p < 0.05; **, p < 0.01; ***, p < 0.001. **b,d,** Associations between CSF MTBR-tau243 and plasma eMTBR-tau243 in BioFINDER-2 cohort (n = 108) (**b**) and the Knight ADRC cohort (n = 55) (**d**). CSF MTBR-tau243 in BioFINDER-2 and the Knight ADRC cohorts were analyzed by the previously reported immunoprecipitation method[19] and the chemical extraction method[23], respectively. In the pilot BioFINDER-2 cohort, green dots color indicates global tau-PET positivity. In the pilot Knight-ADRC cohort, green dots color indicates Aβ-status positivity. For the scatter plots, linear regression lines (solid black) with 95% confidence intervals (shaded area) are also shown. All tests were two-sided. BioFINDER-2 pilot: AD+ vs. CU-: p < 0.001; AD+ vs. MCI + : p = 0.014; Knight-ADRC: AD+ vs CU-: p < 0.001; AD+ vs. CU + : p = 0.001; AD+ vs. very mild AD + : p = 0.005. Abbreviations: Aβ, amyloid β; AD + , Alzheimer's disease dementia Aβ-positive; CU-, cognitively unimpaired Aβ-negative; CU + , cognitively unimpaired Aβ-positive; MCI + , mild cognitive impairment Aβ-positive; MTBR, microtubule-binding region.
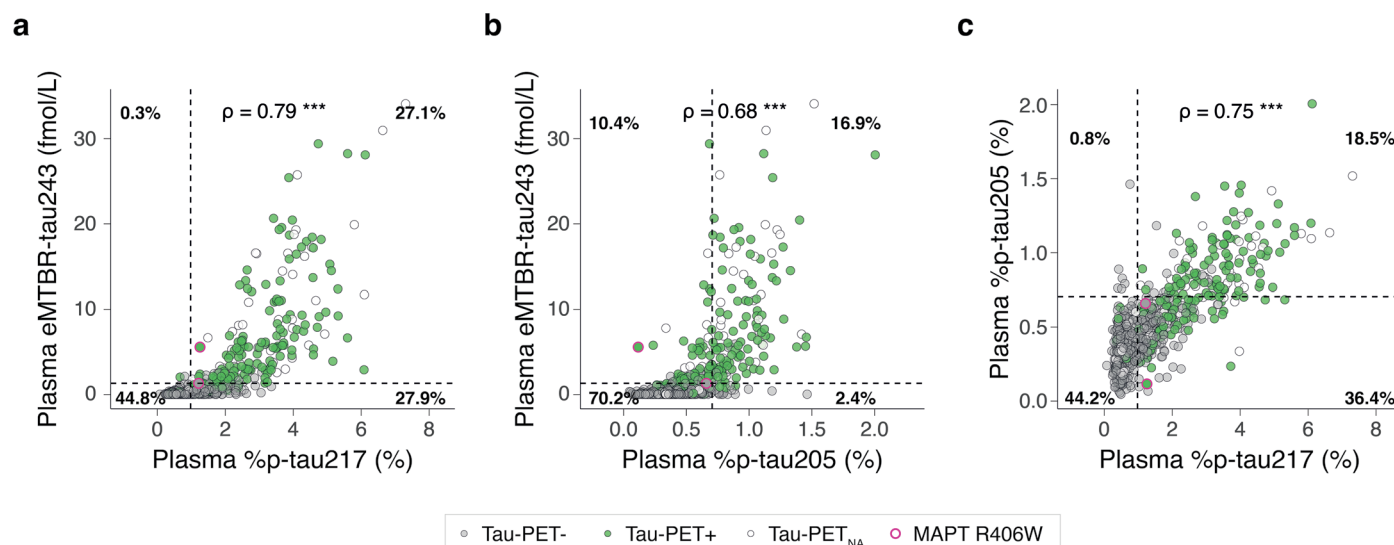
Extended Data Fig. 2 | Cross-correlation among plasma biomarkers in the validation cohort. All individuals with available data are included in these plots. (**a**) Plasma %p-tau217 vs. eMTBR-tau243, (**b**) plasma %p-tau205 vs. eMTBR-tau243, and (**c**) plasma %p-tau217 vs. %p-tau205 are shown. Dots are gray-color-coded to indicate tau-PET negativity in the Global (Braak I-VI) regions of interests (ROI) while white-color-coded dots indicate tau-PET data are not available and other color-coded dots indicate tau-PET positivity. MAPT R406W mutation carriers are shown in pink (one FTD case and one MCI-). Plasma thresholds were derived using Gaussian mixture modelling. Percentage of individuals in each of the four quadrants are shown. Strength of correlation is shown using Spearman's ρ. All tests were two-sided and all p-values < 0.001. ***p:<0.001. Abbreviations: FTD, frontotemporal dementia; MCI-, mild cognitive impairment without Aβ pathology.

a

Global tau-pathology
(Aβ+ participants)

b

Aβ-pathology
(All participants)
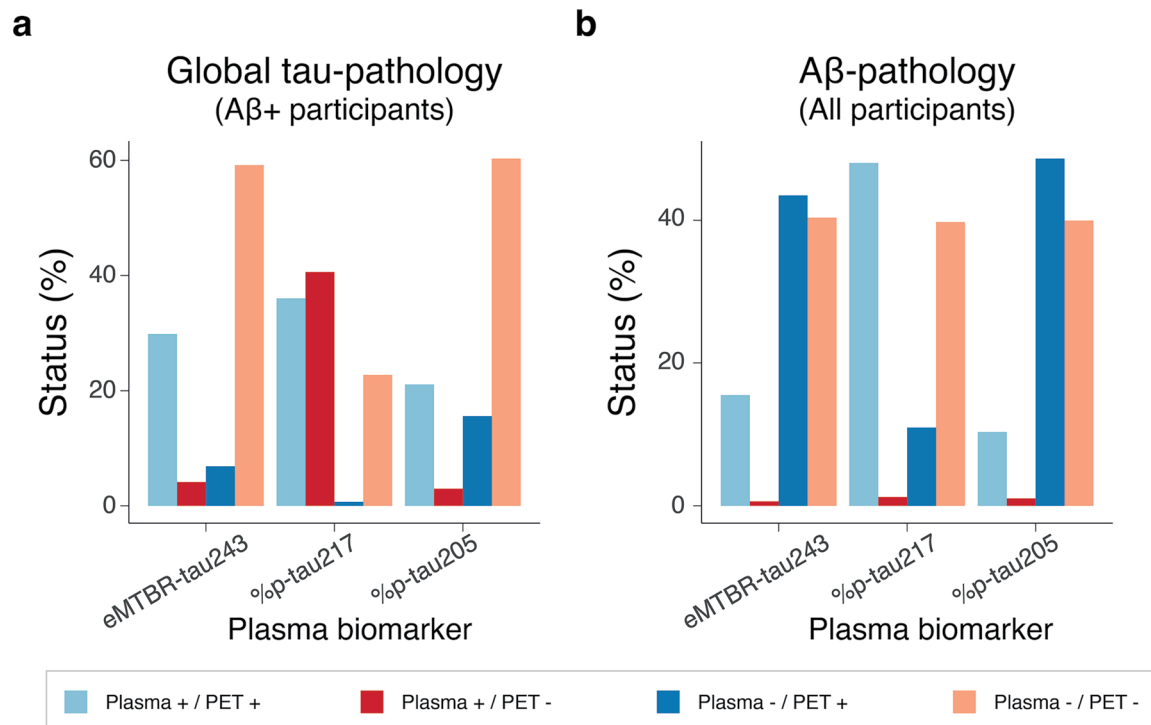
Extended Data Fig. 3 | Relationships between plasma and PET status. Barplots represent the percentage of individuals that were classified in each of the four possible status using plasma and PET dichotomized values. (**a**) Global tau-PET in Aβ-positive participants and (**b**) Aβ-PET in all participants. Plasma thresholds were derived using Gaussian mixture modelling. We used previously validated cutoffs for PET (Aβ: >1.03 SUVR; tau: 1.22 SUVR). For eMTBR-tau243 in Aβ-positive participants, most individuals were negative both on tau-PET and eMTBR-tau243 (59.2%), followed by those positive for both (29.8%), with minimal discordance (tau-PET-positive/eMTBR-tau243-negative: 4.1%; tau-PET-negative/eMTBR-tau243-positive: 6.9%). In contrast, plasma %p-tau217 showed a higher proportion of individuals who were plasma-positive but tau-PET-negative (40.6%), indicating the order to see the abnormality of each tau measures. Abbreviation: SUVR, standardized uptake value ratio.
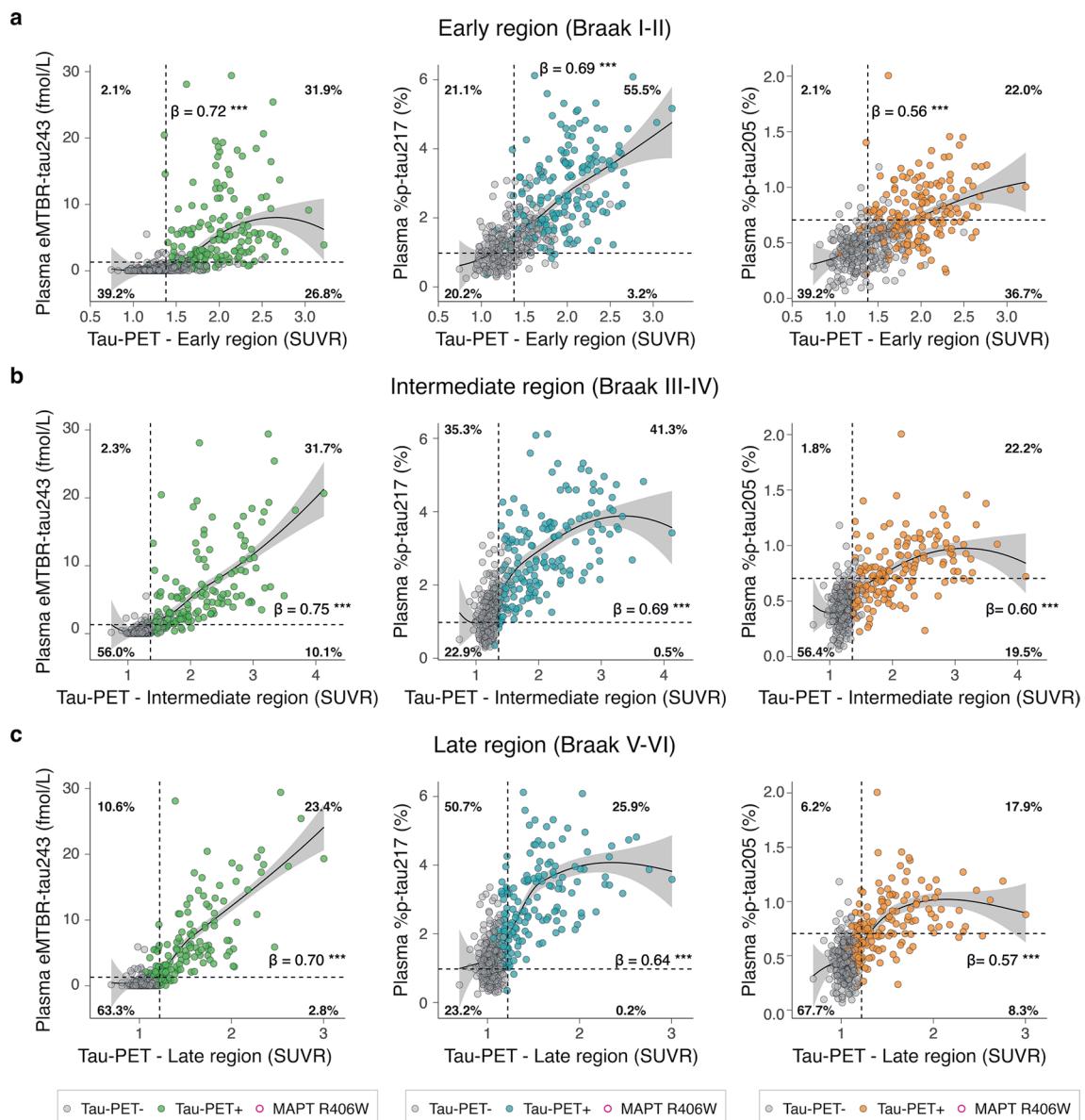
Extended Data Fig. 4 | Association of plasma biomarkers and tau-PET in different regions in Aβ-positive individuals of the validation cohort.
Association of plasma biomarkers and tau-PET in early region (Braak I-II) (**a**, n = 436), intermediate region (Braak III-IV) (**b**, n = 436), and late region (Braak V-VI) (**c**, n = 436). Only Aβ-positive individuals are included in these plots. Dots are gray-color-coded to indicate tau-PET negativity in the Global (Braak I-VI) regions of interest (ROI) while other color-coded dots indicate tau-PET positivity. MAPT R406W mutation carrie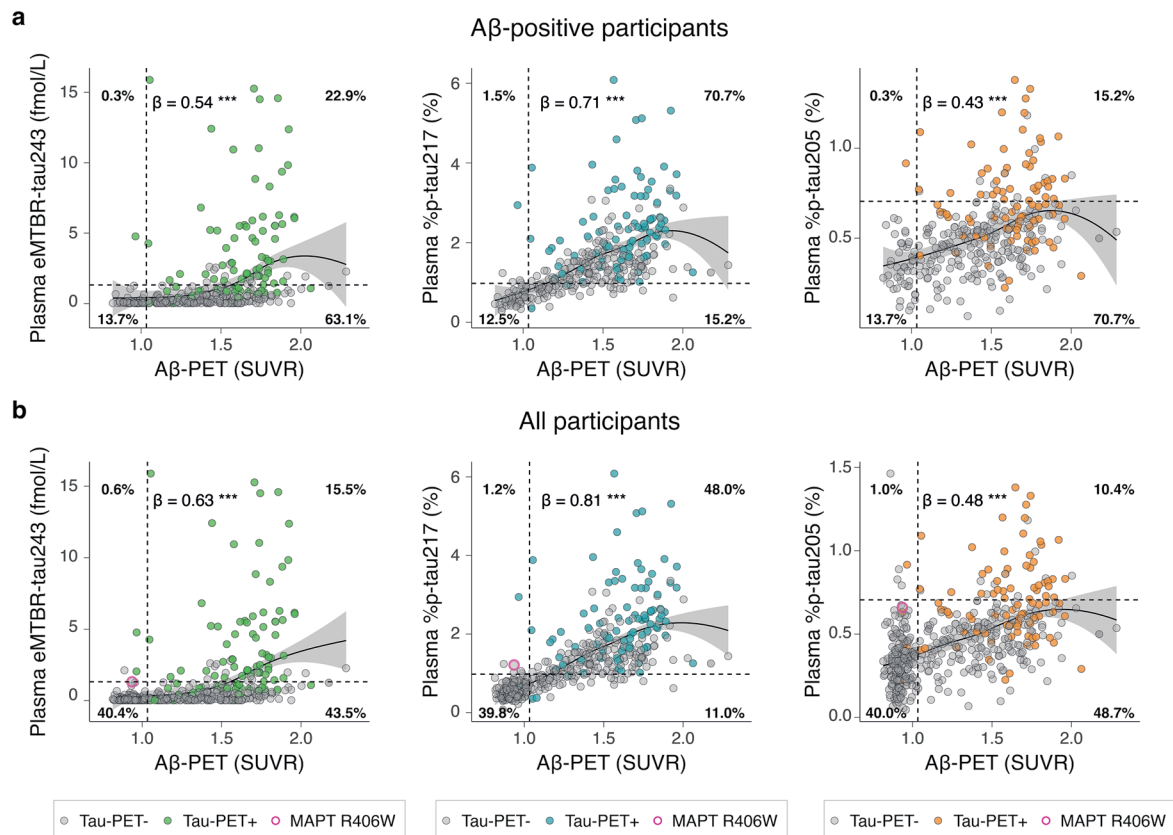rs are shown in pink. Plasma thresholds were derived using Gaussian mixture modelling. Tau-status was assessed using global tau-PET with a previously validated cutoff (SUVR > 1.22). The percentage of individuals in each of the four quadrants is displayed. Standardized β values from linear regression analyses, adjusted for age and sex, are also shown. LOESS trend lines (solid black) with 95% confidence intervals (shaded area) illustrate data tendencies. All tests were two-sided and all p-values < 0.001. ***p:<0.001. Abbreviations: LOESS, locally estimated scatterplot smoothing; SUVR, standardized uptake value ratio.
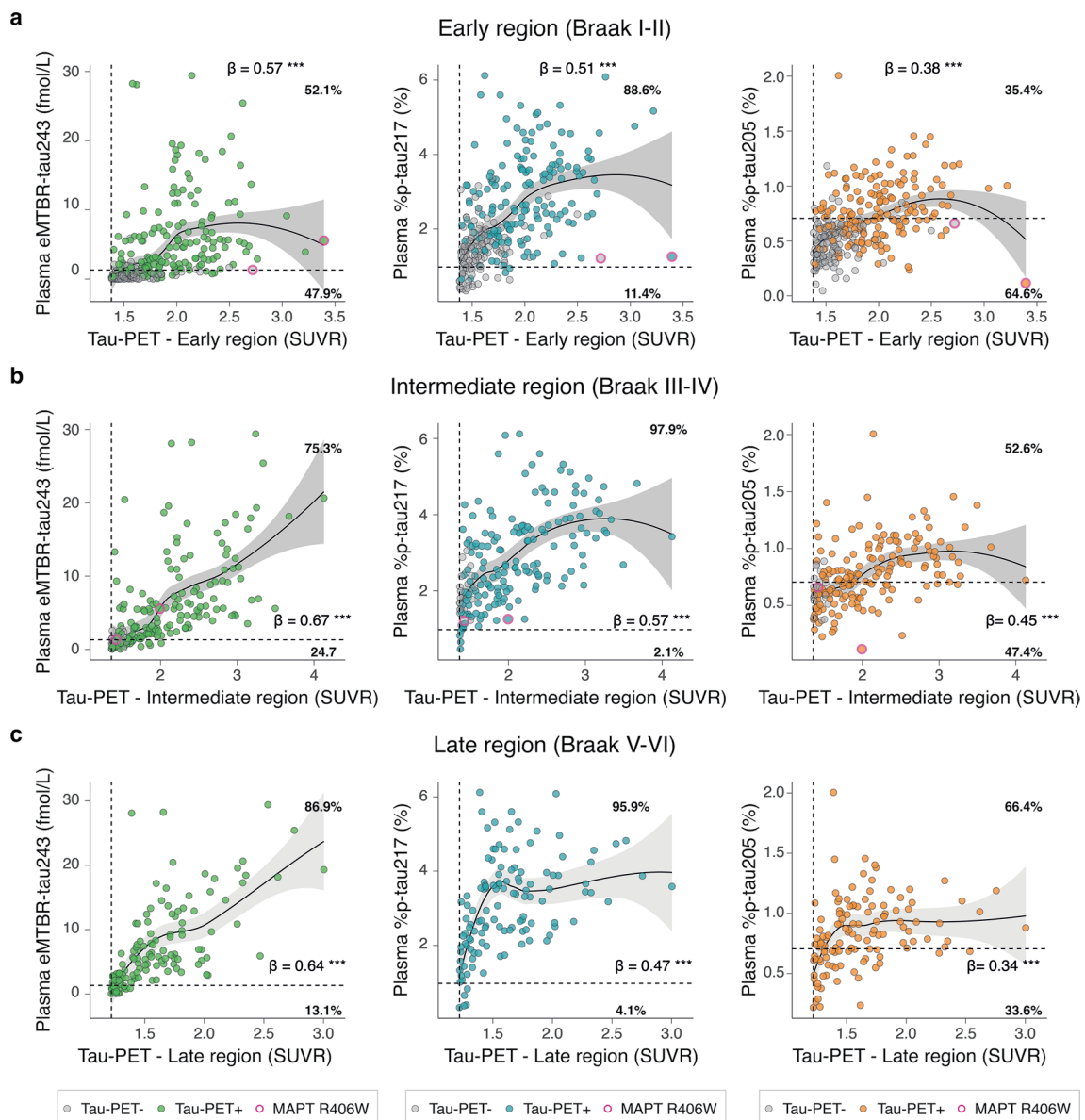
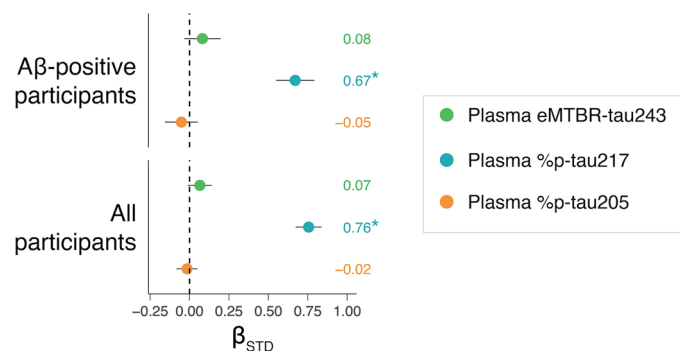**Extended Data Fig. 5 | Association of plasma biomarkers and tau-PET in different regions in tau-PET-positive individuals of the validation cohort.** Association of plasma biomarkers and tau-PET in early region (Braak I-II) (**a**), intermediate region (Braak III-IV) (**b**), and late region (Braak V-VI) (**c**). Only Tau-PET-positive (in each respective region) individuals are included in these plots. Dots are gray-color-coded to indicate tau-PET negativity in the Global (Braak I-VI) regions of interests (ROI) while other color-coded dots indicate tau-PET positivity. MAPT R406W mutation carriers are shown in pink. Plasma thresholds were derived using Gaussian mixture modelling. Global tau-PET status was assessed using global tau-PET with a previously validated cutoff (SUVR > 1.22). The percentage of individuals in each of the four quadrants is displayed. Standardized β values from linear regression analyses, adjusted for age and sex, are also shown. LOESS trend lines (solid black) with 95% confidence intervals (shaded area) illustrate data tendencies. All tests were two-sided. All p-values were <0.001. ***p:<0.001. Abbreviations: LOESS, locally estimated scatterplot smoothing; SUVR, standardized uptake value ratio.
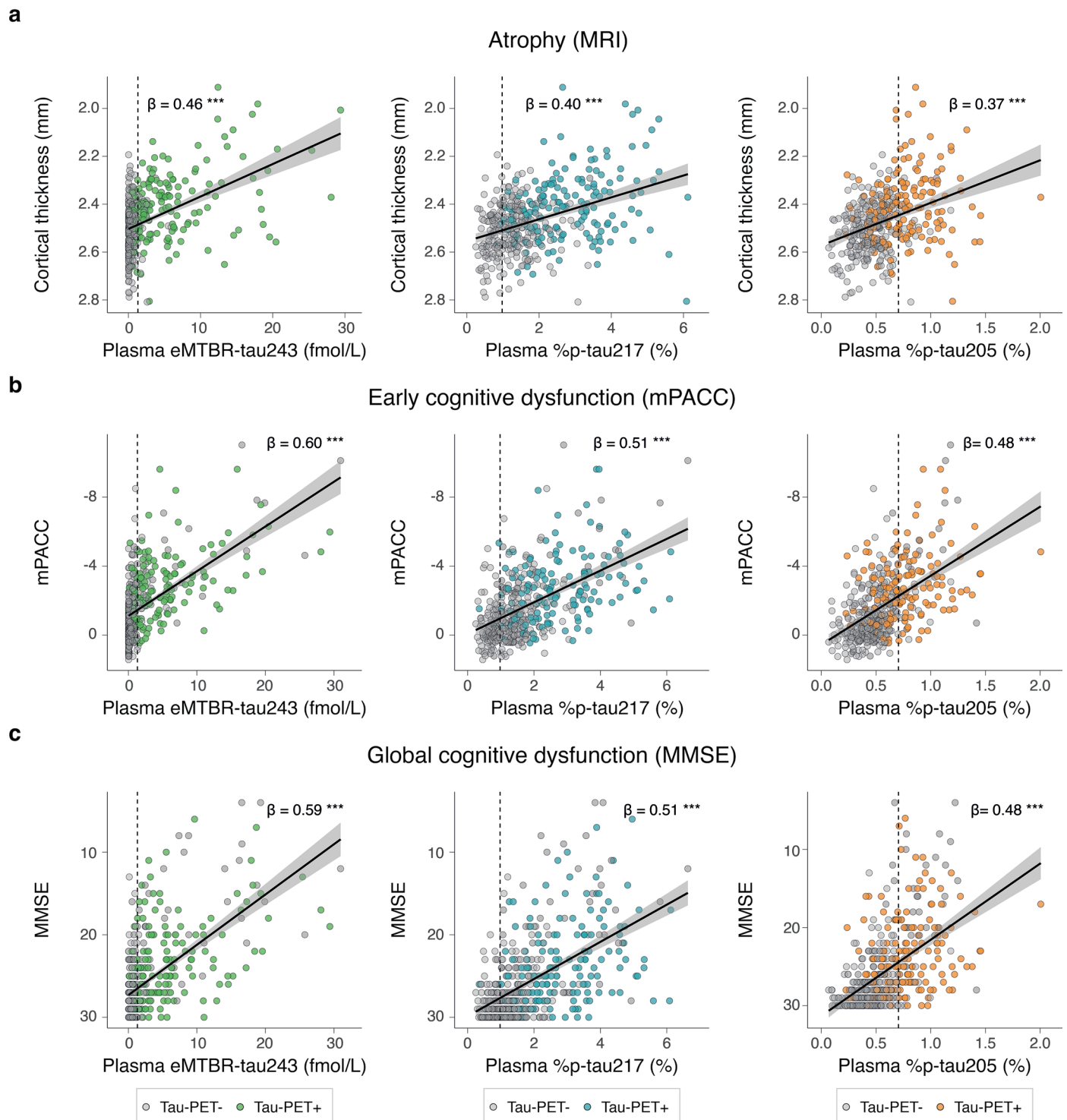
Extended Data Fig. 6 | Association of plasma biomarkers and Aβ-PET in the validation cohort. Only Aβ-positive individuals (**a**) and all individuals (**b**) with available data are included in the scatter plots. Dots are gray-color-coded to indicate tau-PET negativity in the Global (Braak I-VI) regions of interests (ROI) while other color-coded dots indicate tau-PET positivity. MAPT R406W mutation carriers are shown in pink. Plasma thresholds were derived using Gaussian mixture modelling. We used previously validated cutoffs for Aβ-PET (SUVR > 1.03). Tau-status was assessed using global tau-PET (SUVR > 1.22). The percentage of individuals in each of the four quadrants is displayed. Standardized β values from linear regression analyses, adjusted for age and sex, are also shown. LOESS trend lines (solid black) with 95% confidence intervals (shaded area) illustrate data tendencies. All tests were two-sided and all p-values < 0.001. ***p:<0.001. Abbreviations: LOESS, locally estimated scatterplot smoothing; SUVR, standardized uptake value ratio.

Extended Data Fig. 7 | Multivariate analysis of association between plasma biomarkers and Aβ-PET in the validation cohort. Forest plots represent standardized β (dot) and 95%CI (black lines) from a multivariate model including all three plasma biomarkers as predictors and continuous Aβ-PET as the outcome. The analyzed groups are listed on the left (Aβ-positive: n = 328; all: n = 483). Models were adjusted for age and sex. Vertical dotted lines indicate zero. Asterisks represent significant effect (p < 0.05) for each biomarker and model. Aβ-status was assessed using CSF Aβ42/40 or Aβ-PET. All tests were two-sided. Specific p-values can be found in Supplementary Table 5.

a

Atrophy (MRI)

b

Early cognitive dysfunction (mPACC)

c

Global cognitive dysfunction (MMSE)

Extended Data Fig. 8 | Association of plasma biomarkers with brain atrophy and cognition in Aβ-positive individuals of the validation cohort. We show associations between each plasma biomarker and brain atrophy, as measured as cortical thickness (**a**), and early (**b**) and global (**c**) cognitive dysfunction, measured by mPACC and MMSE, respectively. Only Aβ-positive individuals are included in these plots. Dots are gray-color-coded to indicate tau-PET negativity in the Global (Braak I-VI) regions of interests (ROI) while other color-coded dots indicate tau-PET positivity. Tau-status was assessed using global tau-PET with a previously validated cutoff (SUVR > 1.22). Plasma thresholds were derived using Gaussian mixture modelling. Standardized β from linear regression analyses are also shown, adjusting for age and sex (and education for cognitive outcomes). Trend lines (solid black) with 95% confidence intervals (shaded area) from linear regression models illustrate data tendencies. All tests were two-sided and all p-values < 0.001. ***p:<0.001. Abbreviations: mPACC, modified preclinical Alzheimer's cognitive composite; MMSE, Mini-Mental State Examination; SUVR, standardized uptake value ratio.
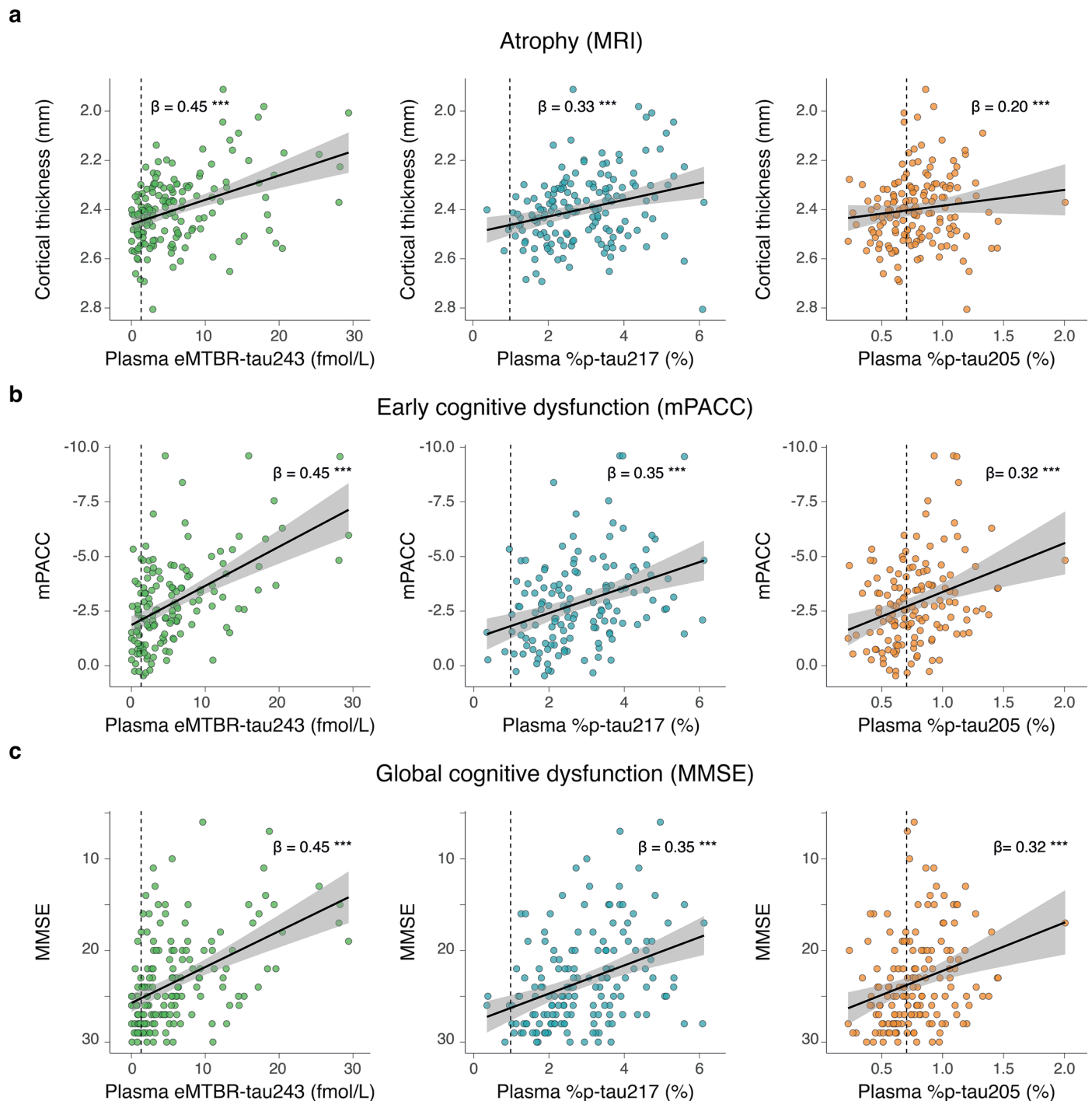
Extended Data Fig. 9 | Association of plasma biomarkers with brain atrophy and cognition in tau-PET-positive individuals of the validation cohort. We show associations between each plasma biomarker and atrophy (**a**), as measured as cortical thickness, and early (**b**) and global (**c**) cognitive dysfunction, measured by mPACC and MMSE, respectively. Only global tau-PET-positive individuals are shown here. Tau-status was assessed using global tau-PET with a previously validated cutoff (SUVR > 1.22). Plasma thresholds were derived using Gaussian mixture modelling. Standardized β from linear regression analyses are also shown, adjusting for age and sex (and education for cognitive outcomes). Linear regression lines (solid black) with 95% confidence intervals (shaded area) are also shown. All tests were two-sided. All p-values were <0.001. ***p:<0.001. Abbreviations: mPACC, modified preclinical Alzheimer's cognitive composite; MMSE, Mini-Mental State Examination; SUVR, standardized uptake value ratio.

Corresponding author(s): Kanta Horie, Oskar Hansson, Randall J. Bateman

Last updated by author(s): Feb 25, 2025

Reporting Summary

Nature Portfolio wishes to improve the reproducibility of the work that we publish. This form provides structure for consistency and transparency in reporting. For further information on Nature Portfolio policies, see our Editorial Policies and the Editorial Policy Checklist.

Statistics

For all statistical analyses, confirm that the following items are present in the figure legend, table legend, main text, or Methods section.

n/a	Confirmed	
☐	☒	The exact sample size (*n*) for each experimental group/condition, given as a discrete number and unit of measurement
☐	☒	A statement on whether measurements were taken from distinct samples or whether the same sample was measured repeatedly
☐	☒	The statistical test(s) used AND whether they are one- or two-sided *Only common tests should be described solely by name; describe more complex techniques in the Methods section.*
☐	☒	A description of all covariates tested
☐	☒	A description of any assumptions or corrections, such as tests of normality and adjustment for multiple comparisons
☐	☒	A full description of the statistical parameters including central tendency (e.g. means) or other basic estimates (e.g. regression coefficient) AND variation (e.g. standard deviation) or associated estimates of uncertainty (e.g. confidence intervals)
☐	☒	For null hypothesis testing, the test statistic (e.g. F, t, r) with confidence intervals, effect sizes, degrees of freedom and P value noted *Give P values as exact values whenever suitable.*
☒	☐	For Bayesian analysis, information on the choice of priors and Markov chain Monte Carlo settings
☒	☐	For hierarchical and complex designs, identification of the appropriate level for tests and full reporting of outcomes
☒	☐	Estimates of effect sizes (e.g. Cohen's *d*, Pearson's *r*), indicating how they were calculated

Our web collection on statistics for biologists contains articles on many of the points above.

Software and code

Policy information about availability of computer code

Data collection	LC-MS experiments were performed using nanoAcquity UPLC system (Waters, Mildford, MA) coupled to Orbitrap Eclipse mass spectrometer (Thermo Scientific, San Jose, CA).
Data analysis	MS transitions peaks were extracted and quantified using Xcalibur software version 3.0.63 (Thermo Scientific). Statistical analyses were conducted using R version 4.1.0. pROC package (v1.18.4) was used.

For manuscripts utilizing custom algorithms or software that are central to the research but not yet described in published literature, software must be made available to editors and reviewers. We strongly encourage code deposition in a community repository (e.g. GitHub). See the Nature Portfolio guidelines for submitting code & software for further information.

Data

Policy information about availability of data

All manuscripts must include a data availability statement. This statement should provide the following information, where applicable:

- Accession codes, unique identifiers, or web links for publicly available datasets
- A description of any restrictions on data availability
- For clinical datasets or third party data, please ensure that the statement adheres to our policy

The datasets generated and/or analyzed during the current study are available from the corresponding authors (K.H., R.J.B and O.H). Research participant privacy protection is necessary for controlled access. We will share datasets within the restrictions of IRB ethics approvals, upon reasonable request. Pseudonymized data

Research involving human participants, their data, or biological material

Policy information about studies with [human participants or human data](). See also policy information about [sex, gender (identity/presentation), and sexual orientation]() and [race, ethnicity and racism]().

Reporting on sex and gender	Sex and gender were self-identified.
Reporting on race, ethnicity, or other socially relevant groupings	Race and ethnicity were not identified in this study because of the policy in BioFINDER-2 study.
Population characteristics	Population characteristics are described in Table 1, Supplementary Data Table 1 and 2. In the pilot BioFINDER-2 cohort (n=108), participants were divided in cognitively unimpaired (CU) either Amyloid-negative or positive (CU- [n=57] and CU+ [n=4], respectively), mild cognitive impairment Amyloid-positive (MCI+) (n=10), and AD dementia Amyloid-positive (AD+) (n=37). In the pilot Knight ADRC cohort (n=55), participants were divided in CU- (n=15) and CU+ (n=14) with Clinical Dementia Rating (CDR)=0, very mild AD dementia (CDR=0.5) Amyloid-positive (n=18), or AD+ with CDR≥1 (n=8). In the BioFINDER-2 validation cohort (n=739), participants were divided in CU- (n=110), CU+ (n=198), MCI+ (n=169), AD+ (n=134), Parkinson's disease or Lewy Body dementia (n=18), progressive supranuclear palsy or corticobasal syndrome (n=6), vascular dementia (n=4), frontotemporal dementia (n=2), R406W MAPT mutation carriers (n=2), MCI without Amyloid-positive (MCI-) (n=86), and other neurodegenerative dementia (n=12).
Recruitment	BioFINDER-2 cohort included cognitively unimpaired participants (recruited as cognitively normal controls or as subjective cognitive decline [SCD] patients), patients with MCI, AD dementia patients and patients with a non-AD neurodegenerative disease. Participants were recruited at Skåne University Hospital and the Hospital of Ängelholm in Sweden. Details on recruitment, exclusion and inclusion criteria have been presented before (reference 11). The Knight ADRC cohort consisted of community-dwelling volunteers enrolled in studies of memory and aging at Washington University in St. Louis. Knight ADRC participants underwent the Clinical Dementia Rating (CDR) test. Individuals with a CDR of 0.5 or greater were considered to have a dementia syndrome and the probable aetiology of the dementia syndrome was formulated by clinicians based on clinical features in accordance with standard criteria and methods.
Ethics oversight	All participants in the Swedish BioFINDER-2 and the Knight ADRC cohorts gave written informed consent and ethical approvals were granted by the Regional Ethical Committee in Lund, Sweden and the Washington University Human Research Protection Office, respectively.

Note that full information on the approval of the study protocol must also be provided in the manuscript.

Field-specific reporting

Please select the one below that is the best fit for your research. If you are not sure, read the appropriate sections before making your selection.

☒ Life sciences   ☐ Behavioural & social sciences   ☐ Ecological, evolutionary & environmental sciences

For a reference copy of the document with all sections, see [nature.com/documents/nr-reporting-summary-flat.pdf]()

Life sciences study design

All studies must disclose on these points even when the disclosure is negative.

Sample size	No statistical methods were used to pre-determine sample size but our sample size is similar or larger to that used for similar studies. (e.g., Horie, K., et al. Nat Med 29, 1954-1963 (2023) and Barthelemy, N.R., et al. Nat Med 26, 398-407 (2020))
Data exclusions	No data points were excluded from analyses; outliers were not removed.
Replication	We replicated our key findings in two pilot cohorts (pilot BioFINDER-2 and pilot Knight ADRC) and a large validation cohort (BioFINDER-2 validation cohort).
Randomization	Samples were randomized by groups such as cognitively unimpaired participants, patients with MCI, AD dementia patients and patients with a non-AD neurodegenerative disease. All samples had a random code as an identifier and researchers who performed experiments were blinded towards the code when performing the analyses.
Blinding	All assays and data extraction steps were performed by operators blinded to any clinical or biomarker information.

Reporting for specific materials, systems and methods

We require information from authors about some types of materials, experimental systems and methods used in many studies. Here, indicate whether each material, system or method listed is relevant to your study. If you are not sure if a list item applies to your research, read the appropriate section before selecting a response.

Materials & experimental systems

n/a	Involved in the study
☐	☒ Antibodies
☒	☐ Eukaryotic cell lines
☒	☐ Palaeontology and archaeology
☒	☐ Animals and other organisms
☐	☒ Clinical data
☒	☐ Dual use research of concern
☒	☐ Plants

Methods

n/a	Involved in the study
☒	☐ ChIP-seq
☒	☐ Flow cytometry
☒	☐ MRI-based neuroimaging

Antibodies

Antibodies used	HJ32.11 antibody (generated by Dr. David Holtzman) was used. For the purification of eMTBR-tau243 in plasma, the HJ32.11 antibody was coupled to sepharose beads at 3 mg/gram, and the beads with 45 micro-gram HJ32.11 antibody was added per sample (1.4 mL plasma).
Validation	HJ32.11 was validated in the following study. Horie, K. et al. CSF MTBR-tau243 is a specific biomarker of tau tangle pathology in Alzheimer's disease. Nat Med 29, 1954–1963 (2023).

Clinical data

Policy information about clinical studies

All manuscripts should comply with the ICMJE guidelines for publication of clinical research and a completed CONSORT checklist must be included with all submissions.

Clinical trial registration	BioFINDER-2 (NCT03174938) Knight ADRC (N/A--the study is NOT a clinical trial)
Study protocol	BioFINDER-2 (NCT03174938, https://clinicaltrials.gov/ct2/show/NCT03174938) Knight ADRC (N/A--the study is NOT a clinical trial)
Data collection	Data was obtained from plasma collected from participants in the BioFINDER-2 cohort (NCT03174938) including cognitively unimpaired participants, patients with MCI, AD dementia patients and patients with a non-AD neurodegenerative disease. Participants in the Knight ADRC cohort were community-dwelling volunteers enrolled in studies of memory and aging.
Outcomes	Secondary outcome measures including the change on plasma tau biomarkers measured by mass spectrimetry were obtained in this study.

Plants

Seed stocks	N/A
Novel plant genotypes	N/A
Authentication	N/A